NAVAL POSTGRADUATE SCHOOL
Monterey, California

THESIS

EFFECTS OF NON-UNIFORM WINDOWING ON THE PERFORMANCE OF A FAST FREQUENCY-HOPPED NONCOHERENT MFSK RECEIVER OVER RICIAN FADING CHANNELS WITH PARTIAL-BAND INTERFERENCE AND DOPPLER SHIFT

by

Thomas W. Vece

June, 1991

Thesis Advisor: R. Clark Robertson
Co-Advisor: Tri T. Ha

UNCLASSIFIED
SECURITY CLASSIFICATION OF THIS PAGE

REPORT DOCUMENTATION PAGE

Form Approved
OMB No. 0704-0188

1a REPORT SECURITY CLASSIFICATION UNCLASSIFIED	1b RESTRICTIVE MARKINGS
2a SECURITY CLASSIFICATION AUTHORITY	3 DISTRIBUTION / AVAILABILITY OF REPORT Approved for public release; distribution is unlimited
2b DECLASSIFICATION / DOWNGRADING SCHEDULE	
4 PERFORMING ORGANIZATION REPORT NUMBER(S)	5 MONITORING ORGANIZATION REPORT NUMBER(S)
6a NAME OF PERFORMING ORGANIZATION Naval Postgraduate School 6b OFFICE SYMBOL (If applicable) EC	7a NAME OF MONITORING ORGANIZATION Naval Postgraduate School
6c ADDRESS (City, State, and ZIP Code) Monterey, CA 93943-5000	7b ADDRESS (City, State, and ZIP Code) Monterey, CA 93943-5000
8a NAME OF FUNDING / SPONSORING ORGANIZATION 8b OFFICE SYMBOL (If applicable)	9 PROCUREMENT INSTRUMENT IDENTIFICATION NUMBER
8c ADDRESS (City, State, and ZIP Code)	10 SOURCE OF FUNDING NUMBERS PROGRAM ELEMENT NO / PROJECT NO / TASK NO / WORK UNIT ACCESSION NO

11 TITLE (Include Security Classification) EFFECTS OF NON-UNIFORM WINDOWING ON THE PERFORMANCE OF A FAST FREQUENCY-HOPPED NONCOHERENT MFSK RECEIVER OVER RICIAN FADING CHANNELS WITH PARTIAL-BAND INTERFERENCE AND DOPPLER SHIFT

12 PERSONAL AUTHOR(S)
Vece, Thomas W.

13a TYPE OF REPORT	13b TIME COVERED	14 DATE OF REPORT (Year, Month, Day)	15 PAGE COUNT
Master's Thesis	FROM _____ TO _____	1991, June	63

16 SUPPLEMENTARY NOTATION The views expressed in this thesis are those of the author and do not reflect the official policy or position of the Department of Defense or the U.S. Government

17 COSATI CODES			18 SUBJECT TERMS (Continue on reverse if necessary and identify by block number)
FIELD	GROUP	SUB-GROUP	DFT; MFSK; Rician fading; Doppler shift; partial-band jamming

19 ABSTRACT (Continue on reverse if necessary and identify by block number)

An error probability analysis is done for a DFT based, M-ary frequency-shift keying (MFSK) communications system employing fast frequency-hopped spread spectrum signals. A linear combination procedure refered to as noise-normalization is employed at the receiver to minimize the effects of partial-band interference, which is modeled as additive Gaussian noise. The performance of the receiver is studied as a function of signal Doppler shift and type of windowing used in the DFT.

The use of fast frequency-hopped spread spectrum is found to improve the performance of the DFT based receiver in all but the most severe cases of Doppler shift. The use of a non-uniform window (i.e., a Hamming window) to improve receiver performance is effective only in the presence of large Doppler shifts. The amount of Doppler shift necessary to warrant the use of a non-uniform window depends

20 DISTRIBUTION / AVAILABILITY OF ABSTRACT	21 ABSTRACT SECURITY CLASSIFICATION
☒ UNCLASSIFIED/UNLIMITED ☐ SAME AS RPT ☐ DTIC USERS	UNCLASSIFIED
22a NAME OF RESPONSIBLE INDIVIDUAL R.Clark Robertson	22b TELEPHONE (Include Area Code) (408)-646-2383 22c OFFICE SYMBOL EC/Rc

DD Form 1473, JUN 86 *Previous editions are obsolete*

SECURITY CLASSIFICATION OF THIS PAGE

S/N 0102-LF-014-6603

UNCLASSIFIED

[19] Continued:

on the amount of jamming noise power at the receiver, but is relatively insensitive to the frequency-hop rate used. In general, in the absence of any information concerning the nature of the received signal, a non-uniform window should be used because the performance degradation experienced at small Doppler shifts is insignificant compared to the performance enhancement gained at large Doppler shifts.

Approved for public release; distribution is unlimited.

Effects of Non-Uniform Windowing on the Performance of a Fast Frequency-Hopped Noncoherent MFSK Receiver Over Rician Fading Channels with Partial-Band Interference and Doppler Shift

by

Thomas W. Vece
Lieutenant, United States Navy
B.S., Loyola University of Chicago, 1984

Submitted in partial fulfillment
of the requirements for the degree of

MASTER OF SCIENCE IN ELECTRICAL ENGINEERING

from the

NAVAL POSTGRADUATE SCHOOL
June 1991

Author: _____
Thomas W. Vece

Approved by: _____
R. Clark Robertson, Thesis Advisor

_____
Tri T. Ha, Thesis Co-Advisor

_____
Michael A. Morgan, Chairman
Department of Electrical and Computer Engineering

ABSTRACT

An error probability analysis is done for a DFT based, M-ary frequency-shift keying (MFSK) communications system employing fast frequency-hopped spread spectrum signals. A linear combination procedure referred to as noise-normalization is employed at the receiver to minimize the effects of partial-band interference, which is modeled as additive Gaussian noise. The performance of the receiver is studied as a function of signal Doppler shift and type of windowing function used in the DFT.

The use of fast frequency-hopped spread spectrum is found to improve the performance of the DFT based receiver in all but the most severe cases of Doppler shift. The use of a non-uniform window (i.e., a Hamming window) to improve receiver performance is effective only in the presence of large Doppler shifts. The amount of Doppler shift necessary to warrant the use of a non-uniform window depends on the amount of jamming noise power at the receiver, but is relatively insensitive to the frequency-hop rate used. In general, in the absence of any information concerning the nature of the received signal, a non-uniform window should be used because the performance degradation experienced at small Doppler shifts is insignificant compared to the performance enhancement gained at large Doppler shifts.

TABLE OF CONTENTS

I. INTRODUCTION

A. NON-UNIFORM WINDOWING OF THE DISCRETE FOURIER TRANSFORM

The use of the discrete Fourier transform (DFT) to noncoherently detect signals employing M-ary frequency-shift keying (MFSK) modulation has gained popularity recently due to advances made in high speed digital systems. At the current level of technology, however, the utility of the DFT based receiver remains limited due to the speed of real-time DFT algorithms. Even the performance enhancement obtained by using the fast Fourier transform (FFT) is not sufficient to overcome this limitation. However, certain applications - namely fast frequency-hopped spread spectrum systems - can effectively utilize the DFT receiver because lower data rates frequently correspond to higher immunity to narrowband interference. [Ref. 1:p. 2014]

Problems arise in using the DFT based receiver if the transmitted frequency does not match the assigned frequency of the DFT bin. This situation results when the signal frequency is different than that required by the detector, as when the signal experiences a Doppler shift prior to detection. This leads to a situation where transmitted signal energy falsely contributes to an incorrect DFT frequency sample: a phenomena known as self-induced crosstalk [Ref. 1:p. 2015]. This problem

is not specific to the DFT based receiver. What is unique about this type of receiver is its ability to minimize self-induced crosstalk through the use of non-uniform windows. An example of a DFT based detector experiencing self-induced crosstalk is presented in Fig. 1.1. Figure 1.1(a) depicts the situation where the received frequency is perfectly matched to the first output bin of the detector, while Fig. 1.1(b) shows the results of slightly modifying the received signal's frequency. As can be seen, the magnitude of the bin corresponding to the signal is reduced, while the magnitudes of neighboring bins which represent other frequencies are significantly larger. Large amounts of frequency deviation can easily lead to unacceptable bit error rates.

One method that is used to minimize the effects of self-induced crosstalk involves the use of nonuniform windowing; that is, time-sampled data is not equally weighted. The frequency response of typical nonuniform windows have broader main lobes than do rectangular windows (uniform weighting) but exhibit sharper rolloff characteristics. The sharp rolloff characteristics of nonuniform windows partially compensate for the effects of self-induced crosstalk, but in some cases the existence of a broader main lobe creates distortion where it would not otherwise exist [Ref. 1:p. 2015]. Nonetheless, nonuniform windowing can be used successfully to combat large doppler shifts in low data rate environments as demonstrated in [1] and [2].

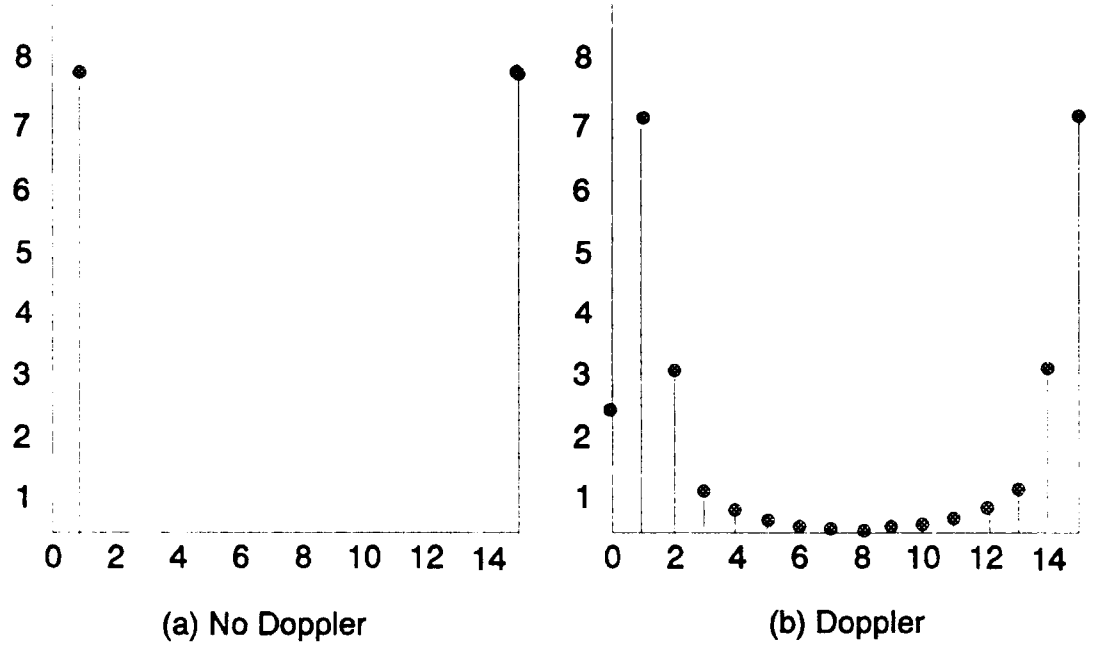

Figure 1.1: Outputs of a DFT (a) without a doppler shifted signal, and (b) with a doppler shifted signal. The adverse effects of a doppler shifted signal can severely degrade communications.

B. FACTORS AFFECTING RECEIVER PERFORMANCE

1. Fast Frequency-Hopping and Partial-Band Interference

When the carrier of the transmitted frequency is changed in an apparently random manner during the transmission of a signal, the overall effect is to spread the energy of the signal over a large bandwidth. This spreading technique is called frequency-hopping and is illustrated in Fig. 1.2. Two types of frequency-hopping are considered: fast and slow frequency-hopping. Slow frequency-hopping systems change, or

hop, the carrier once per data symbol, while fast frequency-hopping systems hop the carrier more than once per data symbol. The higher the hopping rate, the more the frequency spectrum approximates that of true spread spectrum systems utilizing pseudonoise (PN) codes [Ref. 3: pp. 10-14].

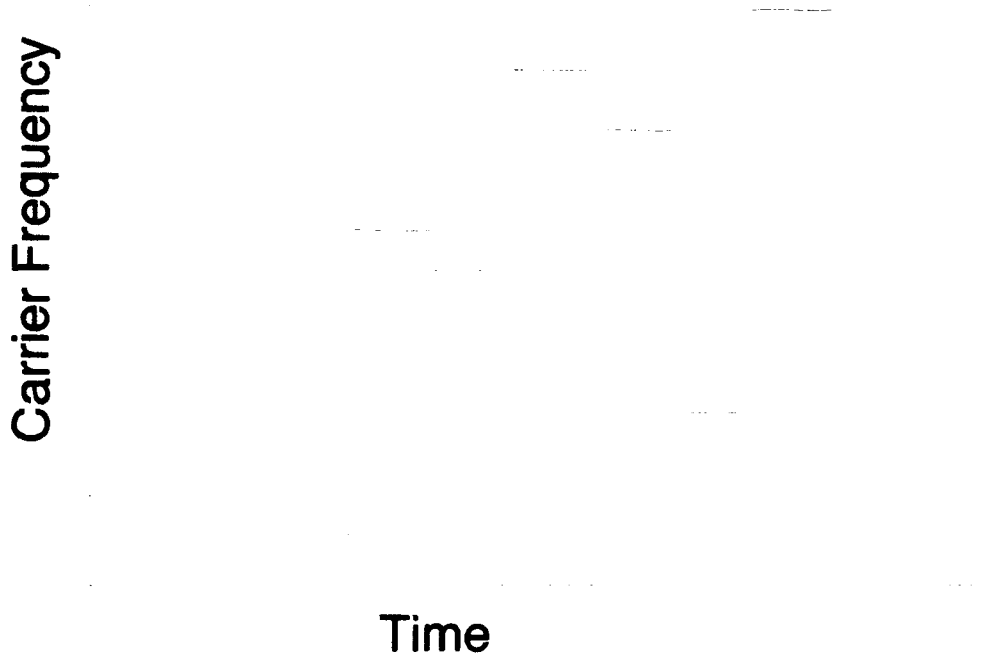

Figure 1.2: An example of hopping the carrier frequency of a signal.

The intent of a hostile jammer is to disrupt communications. In order to effectively jam a frequency-hopped signal, a smart jammer may employ partial-band interference; although, this type of interference can also be caused by other unintended narrowband sources. In utilizing partial-band interference, the jammer concentrates all of the jamming

energy into a fraction of the total bandwidth and randomly hops this signal through the spectrum in the same fashion as the signal employing frequency-hopping. By doing this, the frequency hopped signal cannot always avoid the portion of the spectrum that is jammed; the jammer must be dealt with via the receiver.

The assumptions involved in the analysis to follow are that the jammer is limited in power; that the interference can be modeled as additive Gaussian noise; and that the interference, when present, is present in all detection channels with probability γ. Hence, the probability that interference is not present in any branch is $1-\gamma$. Thus, γ represents the fraction of the spread bandwidth that is jammed. If the partial-band interference is assumed to have a power spectral density of $N_j/2$ over the entire spread bandwidth, the amount of interference present at the receiver due to partial-band interference is $\gamma^{-1}N_j/2$ with probability γ and 0 with probability $1-\gamma$. [Ref. 4:p. 3]

In addition to partial-band interference, the system is assumed to be corrupted by additive white Gaussian noise with a power spectral density of $N_0/2$. Accordingly, the power spectral density of the total noise at the receiver input is $N_0/2+\gamma^{-1}N_j/2$ with probability γ and $N_0/2$ with probability $1-\gamma$. If the receiver equivalent noise bandwidth is W Hz, then the total noise power at the receiver is N_0W with probability $1-\gamma$ and is $(\gamma^{-1}N_j+N_0)W$ with probability γ. [Ref. 4:p. 3]

2. Fading

In addition to partial-band interference, the signal is assumed to be further degraded by fading. Fading is caused by comporents of the signal arriving over different paths which combine to form the total detected signal. Due to the different path lengths traversed by the various signal components, the combined signal amplitude may be greater than or less than the expected amplitude without fading due to constructive and destructive interference. Fading severely degrades the performance of a real world communications system and must be taken into account in any plausible receiver design and analysis.

For this analysis, the signal is assumed to experience slow, frequency non-selective, Rician fading. Slow fading refers to the fact that the amplitude of the signal is assumed to remain constant at least over the duration of one hop, while frequency non-selective implies that all frequency components of the signal experience identical fading. Rician fading is characterized as having a diffuse signal component and a direct signal component. Assumme that the amplitude of the received signal in a Rician fading channel is $a\sqrt{2}$. Then the probabilty density function of the random variable A is given by

$$f_A(a) = \frac{a}{\sigma_f^2} e^{-\left(\frac{a^2+\Gamma^2}{2\sigma_f^2}\right)} I_0\left(\frac{a\Gamma}{\sigma_f^2}\right) u(a), \qquad \textbf{(1)}$$

where $u(\cdot)$ is the unit step function, Γ^2 is the power in the direct component of the signal, $2\sigma_f^2$ is the power in the diffuse component, and $I_0(\cdot)$ is the modified Bessel function of order zero. As can be seen, (1) reduces to the well known Rayleigh distribution when the value of the direct component is zero. [Ref. 5]

C. THE NOISE-NORMALIZED DETECTOR

A noise-normalized detector is a linear receiver that uses the received noise power to normalize the output of each branch before a decision is made regarding which signal is present. This type of receiver is combined with fast frequency hopping to improve overall system immunity to partial-band interference. The noise-normalization is implemented before the hop receptions are combined to form the detection statistics. This type of detection scheme tends to lessen the influence on the overall decision statistic of each hop when interference is present, while increasing the influence of each hop when no interference exists [Ref. 4:p. 2]. Because the output statistics of each branch of the receiver are independent of one another, closed form solutions for the receiver performance can be obtained.

This thesis studies the effects of nonuniform windowing on a noise-normalized DFT based receiver where the signal experiences partial-band interference, Doppler shift, and Rician fading. The effects of fast-frequency hopping the

carrier frequency are analyzed and the results for various hop rates discussed. As in [1] and [2], a statistical analysis is done to determine the amount of frequency deviation necessary to warrant the use of a nonuniform window over a rectangular window.

II. ANALYSIS OF THE NOISE-NORMALIZED DFT BASED DETECTOR

The receiver under consideration is shown in Fig. 2.1. The incoming signal hop is first brought back to baseband and then sampled at the Nyquist rate. The DFT of the signal is computed using the appropriate windowing function and the magnitude of each output bin is squared. Hence, in the absence of both a Doppler shift and a nonuniform window, this receiver is functionally equivalent to a conventional MFSK receiver employing quadratic detectors. At the same time, the total noise power at the receiver is measured, modified appropriately by the windowing function of choice, and inverted to form the noise-normalization term. Each bin output is multiplied by the noise-normalization term. The decision statistics are then obtained by summing over all hops comprising the transmitted symbol. Finally, the detection statistics are compared and the largest one used to determine the estimate of the symbol sent. Errors result when the detection statistic in a channel with no signal is greater than the detection statistic of the signal channel. A detailed analysis of each part of this design follows.

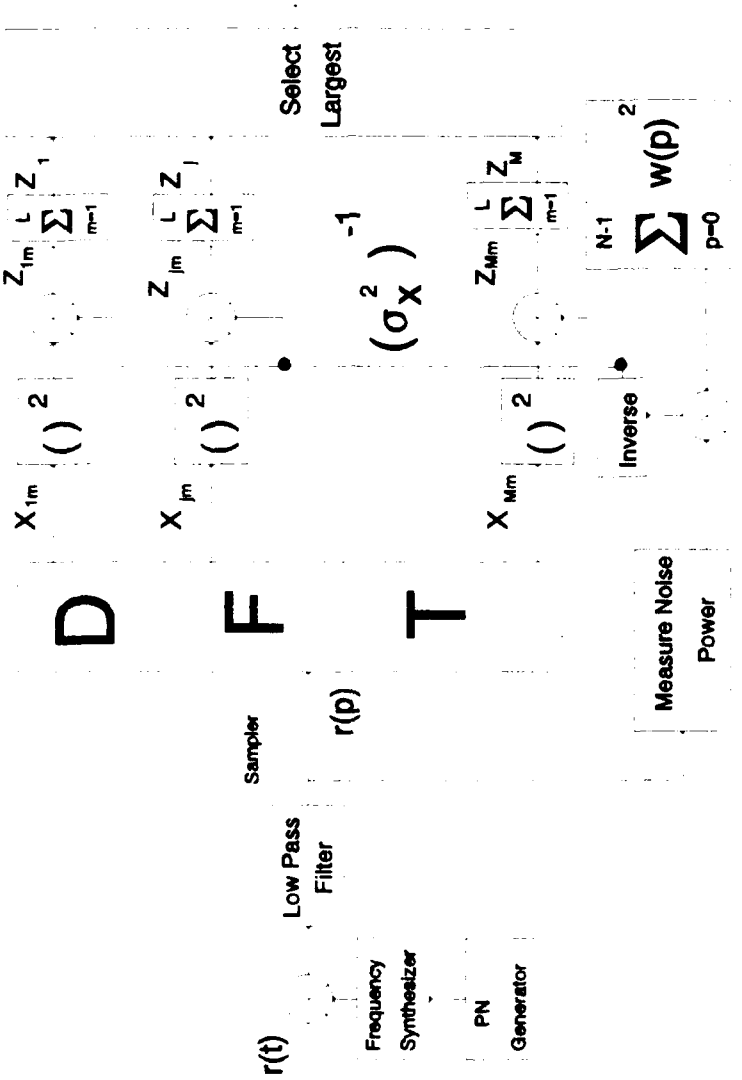

Figure 2.1: The DFT based noise-normalized receiver.

A. DETERMINATION OF THE PROBABILITY DENSITY FUNCTION FOR EACH DFT OUTPUT BIN

The signal input to the receiver in Fig. 2.1 every T_h seconds is of the form

$$r(t) = a\sqrt{2}\cos[2\pi(f_c+f_m+f')t] + n'(t), \quad (2)$$

where $0 \leq t \leq T_h$, a is a Rician random variable having the probability density function of (1), $a\sqrt{2}$ is the Rician distributed signal amplitude, f_c is the carrier frequency hopped every T_h seconds, f_m is the intended symbol frequency, f' is a Doppler shift, and $n'(t)$ is zero mean, additive Gaussian noise. The signal frequencies are chosen to be orthogonal during the time interval $0 \leq t \leq T_h$ and are obtained using the relation

$$f_{m'} = \frac{1}{T_h} + \frac{\Delta_f(m'-1)}{T_h}, \quad (3)$$

where $m' = 1,2,..,M$ and Δ_f is an integer representing the spacing between each of the M signals. To simplify the signal representation, the following substitutions are made:

$$q \triangleq 1 + \Delta_f(m'-1) \quad (4)$$

and

$$\epsilon \triangleq f'T_h \quad (5)$$

so that after the low-pass filter (2) becomes

$$r'(t) = a\sqrt{2}\cos\left[\frac{2\pi(q+\epsilon)t}{T_h}\right] + n(t), \quad \textbf{(6)}$$

where ϵ is the fraction of Doppler shift with respect to the bandwidth of the baseband information signal, q is an integer related to the signal frequency f_m, and $n(t)$ is the filtered noise. The discrete form of the received signal is obtained by using a sampling rate of N/T_h, where N is the number of samples taken during the symbol reception:

$$r(p) = a\sqrt{2}\cos\left[\frac{2\pi(q+\epsilon)p}{N}\right] + n(p), \quad \textbf{(7)}$$

where $p=0,1,..,N-1$ and is the discrete signal sample. [Ref. 2:pp. 7-9]

The output of each bin is a complex quantity and can be separated into real and imaginary parts:

$$Y_m(k|a) = Y_{Rm}(k|a) + jY_{Im}(k|a), \quad \textbf{(8)}$$

where k, which ranges from 0 to $N-1$, is an integer representing the DFT output bin and $Y_m(k|a)$, $Y_{Rm}(k|a)$, and $Y_{Im}(k|a)$ are respectively the DFT output, the real part of the DFT output, and the imaginary part of the DFT output for channel k and frequency hop m conditioned on the Rician distributed random variable a. The real and imaginary parts of the DFT are calculated separately

$$Y_{Rm}(k|a) = \sum_{p=0}^{N-1} r(p)\, w(p) \cos\left[\frac{2\pi kp}{N}\right] = \sum_{p=0}^{N-1} \left[\sqrt{2}a\cos\left[\frac{2\pi(q+\epsilon)p}{N}\right] + n(p)\right] w(p) \cos\left[\frac{2\pi kp}{N}\right], \quad (9)$$

and

$$Y_{Im}(k|a) = \sum_{p=0}^{N-1} r(p)\, w(p) \sin\left[\frac{2\pi kp}{N}\right] = \sum_{p=0}^{N-1} \left[\sqrt{2}a\cos\left[\frac{2\pi(q+\epsilon)p}{N}\right] + n(p)\right] w(p) \sin\left[\frac{2\pi kp}{N}\right], \quad (10)$$

where $w(p)$ represents the windowing function. Assuming slow Rician fading so that the amplitude of the signal remains constant during each hop interval, the conditional probability density function for the random variable X_{km} is

$$f_{X_{km}|A}(x_{km}|a) = \frac{x_{km}}{\sigma_x^2} e^{\frac{-(x_{km}^2+\mu_{km}^2)}{2\sigma_x^2}} I_0\left(\frac{x_{km}\mu_{km}}{\sigma_x^2}\right), \quad (11)$$

where X_{km} is the magnitude of bin k and hop m given by

$$X_{km} = |Y_m(k|a)| = \sqrt{Y_{Rm}(k|a)^2 + Y_{Im}(k|a)^2}, \quad (12)$$

μ_{km} is the magnitude of the expected value of bin k and frequency hop m given by

$$\mu_{km} = |\overline{X_{km}}| = \sqrt{\overline{Y_{Rm}(k|a)}^2 + \overline{Y_{Im}(k|a)}^2}, \quad (13)$$

and σ_x^2 is the variance of bin k given by

$$\sigma_x^2 = \frac{1}{2} E\{|Y_m(k|a) - \overline{Y_m(k|a)}|^2\}. \quad (14)$$

[Ref. 1:p. 2016]

The mean of X_{km} for a fixed amplitude a is easily determined by observing that the only random quantity is $n(p)$ which is zero-mean. This leads to the conclusion that the mean is simply the output of the DFT without noise. The real and imaginary parts of the mean conditioned on a are

$$\underbrace{\overline{Y_{Rm}(k|a)}}_{\triangleq m_{Rm}} = a\sqrt{2}\sum_{p=0}^{N-1} w(p)\cos\left(\frac{2\pi p(q+\epsilon)}{N}\right)\cos\left(\frac{2\pi pk}{N}\right) \qquad \textbf{(15)}$$

and

$$\underbrace{\overline{Y_{Im}(k|a)}}_{\triangleq m_{Im}} = a\sqrt{2}\sum_{p=0}^{N-1} w(p)\cos\left(\frac{2\pi p(q+\epsilon)}{N}\right)\sin\left(\frac{2\pi pk}{N}\right). \qquad \textbf{(16)}$$

An expression for μ_{km}^2 conditioned on a is then determined by substituting (15) and (16) into (13) and squaring both sides:

$$\begin{aligned}\mu_{km}^2 &= m_R^2 + m_I^2 \\ &= a^2(m'^2_R + m'^2_I) \\ &\triangleq a^2\beta_{km}.\end{aligned} \qquad \textbf{(17)}$$

where β_{km} is the magnitude squared of the mean of the DFT output without fading when the signal power is normalized to unity, that is,

$$\begin{aligned}\beta_{km} = 2\Bigg(&\left[\sum_{p=0}^{N-1} w(p)\cos\left(\frac{2\pi p(q+\epsilon)}{N}\right)\cos\left(\frac{2\pi pk}{N}\right)\right]^2 \\ &+\left[\sum_{p=0}^{N-1}\cos\left(\frac{2\pi p(q+\epsilon}{N}\right)\sin\left(\frac{2\pi pk}{N}\right)\right]^2\Bigg).\end{aligned} \qquad \textbf{(18)}$$

[Ref. 2:pp. 10-11]

The variance of X_{km} is obtained by substituting (9), (10), (15), and (16) into (14) and simplifying

$$\begin{aligned}\sigma_x^2 &= \frac{1}{2}E[\,|Y_{Rm}(k|a) - \overline{Y_{Rm}(k|a)} + j\,(Y_{Im}(k|a) - \overline{Y_{Im}(k|a)})\,|^2] \\ &= E[\,|\sum_{p=0}^{n-1} w(p)\,n(p)\cos(\frac{2\pi kp}{N}) \\ &\quad + j\sum_{p=0}^{N-1} w(p)\,n(p)\sin(\frac{2\pi kp}{N})\,|^2]\,.\end{aligned} \tag{19}$$

The magnitude squared of (19) becomes

$$\begin{aligned}\sigma_x^2 &= \frac{1}{2}E[\,(\sum_{p=0}^{N-1} w(p)\,n(p)\cos(\frac{2\pi kp}{N}))^2 \\ &\quad + (\sum_{p=0}^{N-1} w(p)\,n(p)\sin(\frac{2\pi kp}{N}))^2] \\ &= E[\sum_{p=0}^{N-1}\sum_{s=0}^{N-1} w(p)\,w(s)\cos(\frac{2\pi kp}{N})\cos(\frac{2\pi ks}{N})\,n(p)\,n(s) \\ &\quad + \sum_{p=0}^{N-1}\sum_{s=0}^{N-1} w(p)\,w(s)\sin(\frac{2\pi kp}{N})\sin(\frac{2\pi ks}{N})\,n(p)\,n(s)]\,,\end{aligned} \tag{20}$$

where s is an integer having the same range of values as p. Because the expected value operator is a linear operator and the only random quantities are the noise functions, (20) simplifies to

$$\begin{aligned}\sigma_x^2 &= \frac{1}{2}\sum_{p=0}^{N-1}\sum_{s=0}^{N-1} w(p)\,w(s)\cos(\frac{2\pi kp}{N}) \\ &\quad \cdot \cos(\frac{2\pi ks}{N})\,E[n(p)\,n(s)] \\ &\quad + \frac{1}{2}\sum_{p=0}^{N-1}\sum_{s=0}^{N-1} w(p)\,w(s)\sin(\frac{2\pi kp}{N}) \\ &\quad \cdot \sin(\frac{2\pi ks}{N})\,E[n(p)\,n(s)]\,,\end{aligned} \tag{21}$$

The autocorrelation function is defined as

$$R_{nn}(p,s) = E[n(p)\,n(s)]\,, \tag{22}$$

which, because the noise functions represent white noise, is

$$R_{nn}(p,s) = WN_t\delta(p-s)\,, \tag{23}$$

where $\delta(\cdot)$ is the Dirac delta function, W represents the equivalent noise bandwidth of the low-pass filter at the front

of the receiver, and N_t is the power spectral density of the total noise seen at the receiver [Ref. 4]. The quantity N_t equals either N_0 when jamming is not present or N_0+N_j/γ when jamming is present. The expected value needed to solve (21) is obtained by substituting (23) into (22):

$$E[n(p)n(s)] = WN_t\delta(p-s). \tag{24}$$

The final expression for the variance of X_{km} is obtained by substituting (24) into (21) and simplifying:

$$\begin{aligned}
\sigma_x^2 &= \frac{WN_t}{2}\sum_{p=0}^{N-1}\sum_{s=0}^{N-1} w(p)w(s)\cos\left(\frac{2\pi kp}{N}\right)\cos\left(\frac{2\pi ks}{N}\right)\delta(p-s) \\
&+ \frac{WN_t}{2}\sum_{p=0}^{N-1}\sum_{s=0}^{N-1} w(p)w(s)\sin\left(\frac{2\pi kp}{N}\right)\sin\left(\frac{2\pi ks}{N}\right)\delta(p-s) \\
&= \frac{WN_t}{2}\sum_{p=0}^{N-1} w^2(p)\left[\cos^2\left(\frac{2\pi kp}{N}\right)+\sin^2\left(\frac{2\pi kp}{N}\right)\right] \\
&= \frac{WN_t}{2}\sum_{p=0}^{N-1} w^2(p).
\end{aligned} \tag{25}$$

The variance in each bin is affected by both the power spectral density of the external noise and the choice of windowing function used in the DFT.

The probability density function for the output of each bin is found by substituting (17) into (11) and integrating over the range of the Rician distributed amplitude:

$$
\begin{aligned}
f_{X_{km}}(x_{km}) &= \int_0^\infty f_{X_{km}|A}(x_{km}|a)\, f_A(a)\, da \\
&= \int_0^\infty \frac{x_{km}}{\sigma_x^2} e^{\frac{-(x_{km}^2+a^2\beta_{km})}{2\sigma_x^2}} I_0\left(\frac{a x_{km}\sqrt{\beta_{km}}}{\sigma_x^2}\right) \\
&\quad \cdot \frac{a}{\sigma_f^2} e^{\frac{-(a^2+\Gamma^2)}{2\sigma_f^2}} I_0\left(\frac{a\Gamma}{\sigma_f^2}\right) da \\
&= \frac{x_{km}}{\sigma_x^2\sigma_f^2} e^{-\frac{1}{2}\left(\frac{x_{km}^2}{\sigma_x^2}+\frac{\Gamma^2}{\sigma_f^2}\right)} \\
&\quad \cdot \int_0^\infty a e^{-a^2\left(\frac{\beta_{km}}{2\sigma_x^2}+\frac{1}{2\sigma_f^2}\right)} I_0\left(a x_{km}\frac{\sqrt{\beta_{km}}}{\sigma_x^2}\right) I_0\left(\frac{a\Gamma}{\sigma_f^2}\right) da .
\end{aligned}
\tag{26}
$$

By making the substitutions $I_0(x)=J_0(jx)$, and by defining

$$
\begin{aligned}
Q^2 &\triangleq \frac{\beta_{km}}{2\sigma_x^2}+\frac{1}{2\sigma_f^2} \\
&= \frac{\beta_{km}\sigma_f^2+\sigma_x^2}{2\sigma_x^2\sigma_f^2},
\end{aligned}
\tag{27}
$$

and using the integral (from [7])

$$
\int_0^\infty x e^{-Q^2t^2} J_\nu(ax)\, J_\nu(bx)\, dx = \frac{1}{2Q^2} e^{-\left(\frac{a^2+b^2}{4Q^2}\right)} I_\nu\left(\frac{ab}{2Q^2}\right),
\tag{28}
$$

the probability density function is

$$
\begin{aligned}
f_{X_{km}}(x_{km}) &= \frac{x_{km}}{2Q^2\sigma_x^2\sigma_f^2} e^{-\left(\frac{x_{km}^2\sigma_f^2+\Gamma^2\sigma_x^2}{2\sigma_x^2\sigma_f^2}\right)} \\
&\quad \cdot e^{\left(\frac{1}{4Q^2}\right)\left(\frac{x_{km}^2\beta_{km}}{\sigma_x^4}+\frac{\Gamma^2}{\sigma_f^4}\right)} I_0\left(\frac{x_{km}\Gamma\sqrt{\beta_{km}}}{2Q^2\sigma_x^2\sigma_f^2}\right).
\end{aligned}
\tag{29}
$$

The next step involves substituting (27) into (29) which gives

$$f_{X_{km}}(x_{km}) = \left(\frac{x_{km}}{\beta_{km}\sigma_f^2+\sigma_x^2}\right) e^{\frac{-x_{km}^2\sigma_f^2-\Gamma^2\sigma_x^2}{2\sigma_x^2\sigma_f^2} + \frac{x_{km}^2\beta_{km}\sigma_f^4+\Gamma^2\sigma_x^4}{2\sigma_x^2\sigma_f^2(\beta_{km}\sigma_f^2+\sigma_x^2)}} \cdot I_0\left(\frac{x_{km}\Gamma\sqrt{\beta_{km}}}{\beta_{km}\sigma_f^2+\sigma_x^2}\right). \tag{30}$$

Equation (30) simplifies to

$$f_{X_{km}}(x_{km}) = \frac{x_{km}}{\beta_{km}\sigma_f^2+\sigma_x^2} e^{-\frac{1}{2}\left(\frac{x_{km}^2+\beta_{km}\Gamma^2}{\beta_{km}\sigma_f^2+\sigma_x^2}\right)} I_0\left(\frac{x_{km}\Gamma\sqrt{\beta_{km}}}{\beta_{km}\sigma_f^2+\sigma_x^2}\right). \tag{31}$$

In order to clarify the notation, the following substitutions are made:

$$\sigma_{km}^2 \triangleq \beta_{km}\sigma_f^2+\sigma_x^2, \tag{32}$$

and

$$\alpha_{km} \triangleq \Gamma\sqrt{\beta_{km}}. \tag{33}$$

With these substitutions, (31) is seen to be Rician distributed

$$f_{X_{km}}(x_{km}) = \frac{x_{km}}{\sigma_{km}^2} e^{\frac{-(x_{km}^2+\alpha_{km}^2)}{2\sigma_{km}^2}} I_0\left(\frac{x_{km}\alpha_{km}}{\sigma_{km}^2}\right), \tag{34}$$

and reduces to the result obtained in [1] for the case of a nonfading channel ($2\sigma_f^2=0$ and $\Gamma=1$). [Ref. 2:pp. 11-12]

B. ANALYSIS OF THE NOISE-NORMALIZED RECEIVER

1. Determination of the Probability Density Function for the Detection Statistic

As illustrated in Fig. 2.1, the random variable Z_{km} is given by

$$Z_{km}=\frac{X_{km}^{2}}{\sigma_{x}^{2}}, \tag{35}$$

where Z_{km} is the random variable for bin k and frequency hop m. Because all the random variables X_{km} are independent, the transformation of random variables is accomplished by using the relation (from [8])

$$f_{Z_{km}}(z_{km})=\frac{f_{X_{km}}(x_{km(0)})}{g'(x_{km(0)})}, \tag{36}$$

where

$$Z_{km}=g(x_{km}), \tag{37}$$

$g'(x_{km})$ is the derivative of $g(x_{km})$ with respext to x_{km}, and $x_{km(0)}$ is the real root of (35). The denominator in (36) is found by substituting (35) into (37) and differentiating:

$$g'(x_{km(0)}) = \frac{2x_{km(0)}}{\sigma_x^2} = 2\sqrt{\frac{z_{km}}{\sigma_x^2}}. \qquad (38)$$

The transformation of random variables for the noise-normalized detection statistic is determined by substituting (38) into (36):

$$f_{z_{km}}(z_{km}) = \frac{1}{2}\sqrt{\frac{\sigma_x^2}{z_{km}}} f_{x_{km}}(\sqrt{\sigma_x^2 z_{km}}). \qquad (39)$$

The probability density function of z_{km} is obtained by substituting (34) into (39):

$$f_{z_{km}}(z_{km}) = \frac{\sigma_x^2}{2\sigma_{km}^2} e^{\frac{-(\sigma_x^2 z_{km} + \alpha_{km}^2)}{\sigma_{km}^2}} I_0\left(\frac{\alpha_{km}\sigma_x\sqrt{z_{km}}}{\sigma_{km}^2}\right). \qquad (40)$$

The actual detection statistic needed for the comparison is z_k, which is defined as

$$z_k = \sum_{m=1}^{L} z_{km}, \qquad (41)$$

where L is the number of frequency hops per symbol. Since some hops are jammed while others are not, the probability density function of z_k conditioned on the number of jammed hops is simply the multiple convolution of the probability density functions of the jammed and unjammed hops. For instance, if a symbol has three hops and two of them are jammed, the

probability density function of the detection statistic is determined as follows:

$$f_{Z_k}(z_k) = f_{Z_{k1}}(z_{k1})^{jammed} \otimes f_{Z_{k2}}(z_{k2})^{jammed} \otimes f_{Z_{k3}}(z_{k3})^{unjammed}, \quad \textbf{(42)}$$

where $\otimes$ represents convolution. In general, the probability density function of Z_k conditioned on l out of L hops jammed is

$$f_{Z_k}(z_k) = [f_{Z_{km}}(z_{km})^{jammed}]^{\otimes l} \otimes [f_{Z_{km}}(z_{km})^{unjammed}]^{\otimes (L-l)}, \quad \textbf{(43)}$$

where $\otimes c_n$ represents a c_n-fold convolution. [Ref. 4:p. 7]

2. Determining the Probability of Bit Error

Once the random variable transformation is accomplished, the next step involves calculating the probability of bit error. An error will occur if the power in a channel other than the signal channel is greater than the power in the signal channel. Mathematically, this is expressed as

$$Pr(Z_i < Z_j) = \int_0^\infty f_{Z_j}(z_j) \int_0^{z_j} f_{Z_i}(z_i)\, dz_i dz_j, \quad \textbf{(44)}$$

where $i,j=1,\ldots,M$ and $i \neq j$; and the signal is assumed to be in branch i.[Ref. 4: p. 7]. The double integral in (44) determines the probability that the power present in the signal channel is less than the power present in a noise channel.

Because the distribution of power in each noise channel is not identical when Doppler shift is present, the comparison in (44) must be carried out for each noise channel and the results combined to give the total probability of error. An upper bound to the total conditional probability of error is found using the union bound:

$$Ps_{il} \leq \sum_{\substack{j=1 \\ j \neq i}}^{M} Pr(Z_i < Z_j) . \qquad (45)$$

where Ps_{il} is the probability of symbol error given l hops are jammed with the signal present in channel i. [Ref. 1:p. 2017]

Because the distribution of power in each bin varies with the location of the signal, the amount of Doppler, and the relative direction of the frequency shift, an average must be taken over all signal channels and direction of Doppler shift:

$$Ps_l(\epsilon) = \frac{1}{2M} \sum_{i=1}^{M} Ps_{il}(+\epsilon) + Ps_{il}(-\epsilon) , \qquad (46)$$

where $Ps_l(\varepsilon)$ is the total probability of symbol error given l hops are jammed conditioned on the signal experiencing a Doppler shift of ε and $Ps_{il}(\cdot)$ is the probability of symbol error given l hops are jammed with the signal present in channel i conditioned on the signal experiencing a Doppler shift of $(+\varepsilon)$ or $(-\varepsilon)$. The union bound on the conditional probability of symbol error is calculated by combining (45) and (46):

$$Ps_l(\epsilon) \le \frac{1}{2M}\sum_{i=1}^{M}\sum_{\substack{j=1\\ j\neq i}}^{M}\left[Pr(Z_i<Z_j|+\epsilon)+Pr(Z_i<Z_j|-\epsilon)\right]. \qquad (47)$$

The total conditional probability of symbol error assuming l hops are jammed is calculated by combining (44) with (47):

$$Ps_l(\epsilon) \le \frac{1}{2M}\sum_{i=1}^{M}\sum_{\substack{j=1\\ j\neq i}}^{M}\left[\int_0^{\infty} f_{Z_j|+\epsilon}(z_j|+\epsilon)\int_0^{z_j} f_{Z_i|+\epsilon}(z_i|+\epsilon)\,dz_i dz_j \right. \qquad (48)$$
$$\left. +\int_0^{\infty} f_{Z_j|-\epsilon}(z_j|-\epsilon)\int_0^{z_j} f_{Z_i|-\epsilon}(z_i|-\epsilon)\,dz_i dz_j\right].$$

[Ref. 1:p. 2017]

The total probability of symbol error for the noise-normalizing receiver in the presence of partial-band interference is

$$Ps(\epsilon) = \sum_{l=0}^{L}\binom{L}{l}\gamma^l(1-\gamma)^{L-l}Ps_l(\epsilon), \qquad (49)$$

where $Ps(\varepsilon)$ is the total probability of symbol error [Ref. 4:p. 6]. To determine the worst case probability of symbol error, (49) is evaluated for different values of γ, the results compared, and the highest conditional probability of symbol error recorded. The worst case probability of bit error is:

$$Pb(\epsilon) = \frac{M/2}{M-1}Ps(\epsilon), \qquad (50)$$

where $Pb(\varepsilon)$ is the probability of bit error.

An exact solution for the conditional probability of symbol error is calculated by evaluating the probability of not making an error (i.e., the probability that the power in

all noise channels is less than the power in a signal channel):

$$Pr(Z_j<Z_i)=\int_0^{\infty} f_{Z_i}(z_i)\int_0^{z_i} f_{Z_j}(z_j)\,dz_j dz_i. \tag{51}$$

The total conditional probability of not making an error is found by the following relation:

$$\begin{aligned}\overline{Ps_{il}(\epsilon)} &= \prod_{\substack{j=1\\ j\neq i}}^{M} Pr(Z_j<Z_i|\epsilon)\\ &= \prod_{\substack{j=1\\ j\neq i}}^{M} \int_0^{\infty} f_{Z_i}(z_i|\epsilon)\int_0^{z_i} f_{Z_j}(z_j|\epsilon)\,dz_j dz_i,\end{aligned} \tag{52}$$

where $\overline{Ps_{il}(\varepsilon)}$ is the probability of not making an error given that the signal in channel i with l hops jammed and the signal experiencing a Doppler shift of ε. The probability of making an error given that the signal is in channel i with l hops jammed is then given by

$$Ps_{il}(\epsilon)=1-\overline{Ps_{il}(\epsilon)}. \tag{53}$$

which is then used in (46), (47), (48), (49), and (50) to obtain the exact probability of bit error. Due to the enormous amount of computing power needed to numerically integrate (51) and the desire to compare the results with those obtained in [1] and [2], the conditional probability of error based on the union bound was chosen for this thesis.

III. NUMERICAL PROCEDURE

A. PARAMETERIZATION OF VARIABLES

In order to compare the performance of the noise-normalizing receiver with a conventional DFT/MFSK receiver, the number of points used in the DFT, the cut-off frequency of the low pass filter, and the spacing between the M signals are chosen to be consistent with those used in [1] and [2]. The following definitions result from adopting these conventions:

$$N \triangleq 4M, \tag{54}$$

$$W \triangleq 2M, \tag{55}$$

and

$$\Delta_f \triangleq 2, \tag{56}$$

where N is the number of signal samples per hop, M is the modulation order, W is the effective noise bandwidth, and Δ_f is an integer representing the message frequency spacing.

A hop time, T_h, of one second results from sampling the received signal at the Nyquist rate. When this value of T_h and (56) are substituted into (3), it is determined that f_m consists only of odd values ranging from 1 to $2M$-1. Furthermore, the spacing of frequencies in the DFT is

$$\begin{aligned}\Delta f &= \frac{f_s}{N} \\ &= \frac{4M}{4M} \\ &= 1Hz,\end{aligned} \tag{57}$$

where Δf is the frequency resolution of the DFT [Ref. 9]. Because of these choices one empty bin exists between each possible DFT signal output.

A parameter of concern is the energy-per-bit to thermal noise power spectral density ratio defined as E_b/N_0, where E_b is the transmitted energy per bit. The signal-to-noise ratio, which is a measure of the ratio of signal power to noise power, is defined as

$$SNR \triangleq \frac{\Gamma^2 + 2\sigma_f^2}{N_0 W}. \tag{58}$$

For an M-ary system, symbols are sent instead of bits. The power per symbol is the sum of the power in the direct component and the power in the diffuse component:

$$E_s = (2\sigma_f^2 + \Gamma^2)\, T_s, \tag{59}$$

where E_s is the transmitted energy per symbol and T_s is the symbol duration time related to the hop duration time by

$$T_s = LT_h. \tag{60}$$

The energy-per-symbol is related to the energy-per-bit by

$$E_s = E_b \log_2(M) . \tag{61}$$

All the variables used in this thesis are expressed as per-bit quantities; therefore, a relationship between the energy-per-hop and the energy-per-bit is needed. Because each symbol is comprised of L bits,

$$E_h = \frac{E_s}{L} , \tag{62}$$

where E_h is the energy-per-hop. A relationship between the energy-per-bit to noise power spectral density ratio and the signal-to-noise ratio is obtained by combining (58) with (59)

$$\frac{E_b}{N_0} = \frac{WT_s}{\log_2(M)} SNR. \tag{63}$$

Proper choice of the symbol duration time (i.e., T_s=1) and the equivalent noise bandwidth (i.e., $W=log_2(M)$) gives $E_b/N_0=SNR$. In general, however, these two ratios are not equal and must be kept separate in the receiver analysis.

An expression relating the energy-per-bit to noise power spectral density ratio to the signal-to-noise ratio is obtained by combining (58), (60), and (63) and simplifying:

$$\frac{E_b}{N_0} = \frac{(W)(L)(T_h)}{\log_2(M)} \frac{\Gamma^2 + 2\sigma_f^2}{N_0 W} . \tag{64}$$

For the case of a receiver operating in a jammed environment, N_0 is replaced with N_0+N_j/γ when the hop is jammed and (64) becomes

$$\frac{E_b}{N_0}\left(\frac{1}{1+N_j/(\gamma N_0)}\right)=\frac{\Gamma^2+2\sigma_f^2}{W(N_0+N_j/\gamma)}\frac{(W)(L)(T_h)}{\log_2(M)}. \qquad (65)$$

The relationship between the energy-per-bit to noise power spectral density and the signal-to-noise ratio is a function of the effective noise bandwidth of the system, the number of frequency hops per symbol, the hop duration time, and the level of M-ary signalling used.

Another parameter for analysis is the direct to diffuse ratio

$$DTD\triangleq\frac{\Gamma^2}{2\sigma_f^2}. \qquad (66)$$

The following expressions for the direct and the diffuse signal power components result from combining (65) and (66) and simplifying:

$$\sigma_f^2=\frac{E_h}{2(1+DTD)T_h} \qquad (67)$$

and

$$\Gamma^2=\frac{E_h}{T_h}\left(\frac{DTD}{1+DTD}\right). \qquad (68)$$

In doing this analysis, the values of E_b/N_0, N_j/N_0, γ, W, T_h, and DTD are assumed and used to determine the values of Γ^2 and σ_f^2.

B. CONVOLUTING THE PROBABILITY DENSITY FUNCTIONS

In the case of fast frequency-hopping, the probability density function of the total detection statistic is the L-fold convolution of the probability density functions of the detection statistic of each hop. As shown in (49), the total probability of error represents all possible combinations of jammed and unjammed hops. Based on this, a total of $2M(L+1)$ L-fold convolutions are required for each possible signal branch and for each combination of jamming power and fraction of bandwidth jammed that are studied. These convolutions are not required in the case of slow hopping because the total detection statistic is equal to the detection statistic of the single hop. These multiple convolutions are generated by taking advantage of the properties of the Laplace transform.

The Laplace transform of the probability density function of Z_{im} is

$$\begin{aligned} \mathcal{L}[f_{Z_{im}^{(n)}}(z_{im}^{(n)})] &= F_{Z_{im}^{(n)}}(s) \\ &= \int_0^\infty f_{Z_{im}^{(n)}}(z_{im}^{(n)})\, e^{-sz_{im}^{(n)}}\, dz_{im}^{(n)}, \end{aligned} \tag{69}$$

where n=1,2 and n=1 represents the condition of a jammed hop and n=2 represents the condition of an unjammed hop. The Laplace transform of interest is obtained by substituting (40) into (69)

$$F_{Z_{im}^{(n)}}=\int_0^\infty \frac{\sigma_x^{\,2}}{2\sigma_{im}^{\,2(n)}} e^{\frac{-(\sigma_x^{\,2} z_{im}^{(n)}+\alpha_{im}^{\,2(n)})}{2\sigma_{im}^{\,2(n)}}} I_0\left(\frac{\alpha_{im}^{\,(n)}\sigma_x\sqrt{z_{im}^{(n)}}}{\sigma_{im}^{\,2(n)}}\right) e^{-sz_{im}^{(n)}} dz_{im}^{(n)} \qquad (70)$$
$$=\frac{\sigma_x^{\,2}}{2\sigma_{im}^{\,2(n)}} e^{\frac{-\alpha_{im}^{\,2(n)}}{2\sigma_{im}^{\,2(n)}}} \int_0^\infty e^{-z_{im}^{(n)}\left(s+\frac{\sigma_x^{\,2}}{2\sigma_{im}^{\,2(n)}}\right)} I_0\left(\frac{\alpha_{im}^{\,(n)}\sigma_x\sqrt{z_{im}^{(n)}}}{\sigma_{im}^{2(n)}}\right) dz_{im}^{(n)}.$$

Equation (70) is evaluated by defining

$$B=\frac{j\alpha_{im}^{\,(n)}\sigma_x}{\sigma_{im}^{\,2(n)}}, \qquad (71)$$

and

$$C^2=s+\frac{\sigma_x^{\,2}}{2\sigma_{im}^{2(n)}}, \qquad (72)$$

and making the substitutions $u^2=z_{im}$ and $I_0(x)=J_0(jx)$, and using the integral (from [10])

$$\int_0^\infty e^{-C^2u^2} uJ_0(Bu)\,du=\frac{1}{2C^2} e^{-\frac{B^2}{4C^2}}. \qquad (73)$$

The Laplace transform of interest is

$$F_{Z_{im}^{(n)}}(s)=\frac{\sigma_x^{\,2}}{\Lambda^{(n)}} e^{\frac{-\alpha_{im}^{\,2(n)}s}{\Lambda^{(n)}}}, \qquad (74)$$

where

$$\Lambda^{(n)}=2\sigma_{im}^{\,2(n)}s+\sigma_x^{\,2} \qquad (75)$$

[Ref. 4:p. 6]. The probability density function of Z_i is determined by using the fact that convolution in the time domain translates to multiplication in the s domain:

$$F_{Z_i}(s) = F_{Z_{im}}^{(1)}(s)^{l} F_{Z_{im}}^{(2)}(s)^{L-l}. \tag{76}$$

The probability density function of Z_i is given by

$$f_{Z_i}(z_i) = \mathcal{L}^{-1}\left[\left(F_{Z_{im}^{(1)}}(s)\right)^{l} \left(F_{Z_{im}^{(2)}}(s)\right)^{L-l} \right], \tag{77}$$

where L is the number of hops per symbol, l is the number of jammed hops, and $\mathcal{L}^{-1}$ is the inverse Laplace transform operation. In general, (77) cannot be evaluated in closed form and numerical subroutines are used to determine the inverse Laplace transform at each point.

For the case of all hops jammed or unjammed, (77) reduces to

$$\begin{aligned} f_{Z_i^{(n)}}(z_i^{(n)}) &= \mathcal{L}^{-1}\left[\left(F_{Z_{im}^{(n)}}(s)\right)^{L} \right] \\ &= \int_0^{\infty} \left(F_{Z_{im}^{(n)}}(s)\right)^{L} e^{s z_{im}^{(n)}} ds. \end{aligned} \tag{78}$$

The function in the s domain in (78) is obtained by raising (74) to the L power

$$\left[F_{Z_{im}^{(n)}}(s)\right]^{L} = \left(\frac{\sigma_x^{2}}{2\sigma_{im}^{2(n)} s + \sigma_x^{2}}\right)^{L} e^{-\frac{\alpha_{im}^{2(n)} L s}{2\sigma_{im}^{2(n)} s + \sigma_x^{2}}}. \tag{79}$$

Equation (79) is factored as

$$[F_{Z_{im}^{(n)}}(s)]^{L} = \left(\frac{\sigma_x^2}{2\sigma_{im}^{2(n)}}\right)^{L} e^{-\frac{L\alpha_{im}^{2(n)}}{2\sigma_{im}^{2(n)}}} \cdot \left(s+\frac{\sigma_x^2}{2\sigma_{im}^{2(n)}}\right)^{-L} e^{\frac{L\alpha_{im}^{2(n)}\sigma_x^2/(4\sigma_{im}^{4(n)})}{s+\frac{\sigma_x^2}{2\sigma_{im}^{2(n)}}}} . \quad (80)$$

The needed inverse Laplace transform is obtained by combining the transform property that

$$\mathcal{L}^{-1}[F(s+a)] = e^{-az} f(z), \quad (81)$$

the inverse Laplace transform relation (from [11])

$$\mathcal{L}^{-1}\left[\left(\frac{1}{s}\right)^{L} e^{\frac{b}{s}}\right] = \left(\frac{z}{b}\right)^{\frac{L-1}{2}} I_{L-1}(2\sqrt{bz}), \quad (82)$$

with the substitutions

$$a = \frac{\sigma_x^2}{2\sigma_{im}^{2(n)}}, \quad (83)$$

and

$$b = \frac{L\alpha_{im}^{2(n)}\sigma_x^2}{4\sigma_{im}^{4(n)}}. \quad (84)$$

After simplifying, the resulting closed form expression for this special case is

$$f_{Z_i^{(n)}}(z_i^{(n)}) = \frac{\left(\frac{z}{\Omega^{(n)}}\right)^{\frac{L-1}{2}} \sigma_x^2}{2\sigma_{im}^{2(n)}} e^{\frac{-\sigma_x^2}{2\sigma_{im}^{2(n)}}(z+\Omega^{(n)})} I_{L-1}\left(\frac{\sigma_x^2}{\sigma_{im}^{2(n)}}\sqrt{z\Omega^{(n)}}\right), \quad (85)$$

where I_{L-1} is the modified Bessel function of order L-1 and

$$\Omega^{(n)} = L\frac{\alpha_{im}^{2(n)}}{\sigma_x^2} \tag{86}$$

[Ref. 4:p. 7].

C. NUMERICAL INTEGRATION TECHNIQUES

A double numerical integration is needed to evaluate (48), which can be very time consuming. By taking advantage of the properties of the Laplace transform, the double numerical integration is reduced to a single numerical integration. The amount of computing time needed is greatly reduced since

$$\int_0^{z_j} f_{Z_i}(z_i)\,dz_i = \mathcal{L}^{-1}\left[\frac{1}{s}F_{Z_i}(s)\right] \tag{87}$$

and (76) can be divided by s as needed to carry out the inner numerical integration.

The use of the integration technique illustrated in (87) is the primary reason a union bound solution is calculated instead of an exact solution. As seen in (44), the union bound solution requires implementation of (87) only once. The exact solution, as seen in (51), requires using (87) M-1 times since, for the DFT based receiver, the bins that ideally contain no signal will in general have different probability density functions due to Doppler shift and non-uniform windowing. Although using (87) to integrate the probability density function significantly reduces computing time compared to direct numerical integration, the amount of computing

resources needed to calculate the exact solution is much more than that needed to determine the union bound solution. The fact that only a limited amount of these resources was available to generate results justified the decision to evaluate the union bound solution.

The remaining integration is accomplished using Simpson's rule, which is chosen because of its accuracy as compared with the trapezoidal rule. Figure 3.1 shows how Simpson's rule is applied to integration. By dividing the z-axis into equally spaced elements and evaluating the function at each of these points a close approximation of the integral can be obtained through the relation

$$\int_{z_1}^{z_N} f(z)\,dz \approx \frac{\Delta z}{3}\left(f(z_1)+4f(z_2)+2f(z_3)+4f(z_4)+2f(z_5)+\ldots+4f(z_{N-1})+f(z_N)\right) \qquad (88)$$

where an odd number of points must be used [Ref. 12:p. 350]. By choosing an endpoint, varying the spacing between points, and repeatedly evaluating the integral until no difference is observed between successive iterations, an optimal Δz is obtained. A close approximation to the semi-infinite integral is obtained by using that value of Δz while increasing the value of the upper limit on the integral until no difference is detected between successive iterations.

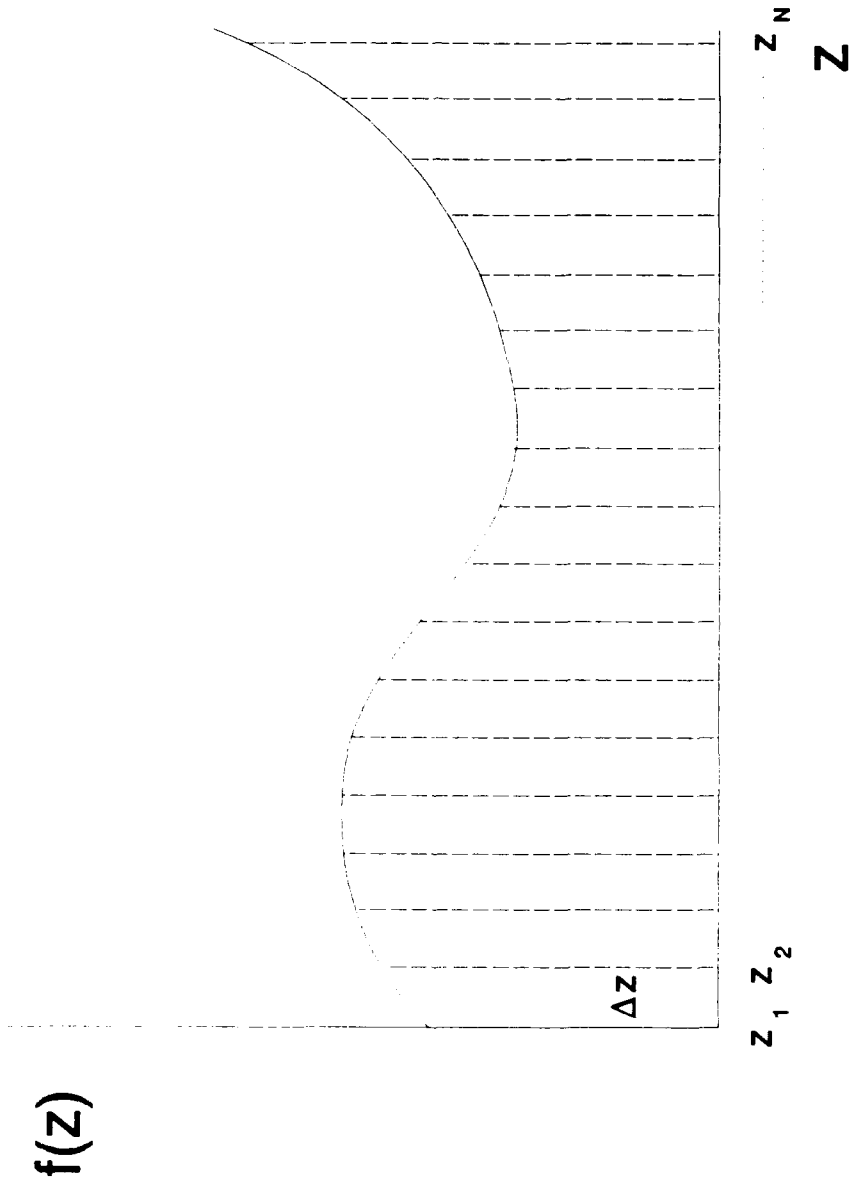

Figure 3.1: Example of dividing a function into equally spaced segments suitable for use with Simpson's rule.

IV. RESULTS

A. PREVIOUS RESULTS

Studies concerning the effects of non-uniform windowing on a DFT based receiver in the presence of a Doppler shifted signal have been performed and documented in [1] and [2]. Each study draws conclusions concerning the effectiveness of the DFT based receiver under different circumstances. The results of these studies are included in order to better understand the conclusions of this thesis.

Reference [1] studies the effects of non-uniform windowing on a DFT based receiver in a nonfading channel with a Doppler shifted signal, where the probability of bit error as a function of the signal-to-noise ratio is obtained. It is demonstrated that using a non-uniform window (specifically, a Hamming window) results in a degradation of performance as compared with the performance of a uniform window for the cases of little of no Doppler shift on the incoming signal. However, performance enhancement is obtained as Doppler shift increases. For the case of M=8, a Doppler shift of ε=.33 is sufficient to warrant the use of non-uniform windowing. Furthermore, the performance improvement increases as the amount of Doppler shift in the signal increases. [Ref. 1: pp. 2017-2018]

The effects of a Rician fading channel on the DFT based receiver are investigated in [2]. Another parameter for analysis is the direct-to-diffuse ratio discussed in the previous chapter. In a manner similar to that developed in [1], data is generated relating the probability of bit error to the signal-to-noise ratio for different direct-to-diffuse ratios. For large direct-to-diffuse ratios (i.e., conditions corresponding to those studied in [1]), the results correlate well. However, as the direct-to-diffuse ratio is decreased, the non-uniform window gives better performance than a rectangular window only when the Doppler shift decreases. The presence of a strong diffuse signal, as illustrated by a small direct-to-diffuse ratio, limits the benefits of using a rectangular window.

B. EFFECTS OF FREQUENCY-HOPPING AND PARTIAL-BAND INTERFERENCE

Graphs of the worst case probability of bit error as a function of signal-to-jamming noise ratio for fixed signal-to-thermal noise ratios are constructed for one, two, three, and four hops per symbol. These results are obtained by numerically evaluating (40), (48), and (49) for values of γ ranging from 1.0 to 0.001 and retaining the worst case performance for each value of E_b/N_j. These results are plotted in Figs. 4.1 through 4.4. The signal-to-noise ratio, direct to diffuse ratio, and the modulation order are chosen to enable direct comparisons with the results obtained in [4] which

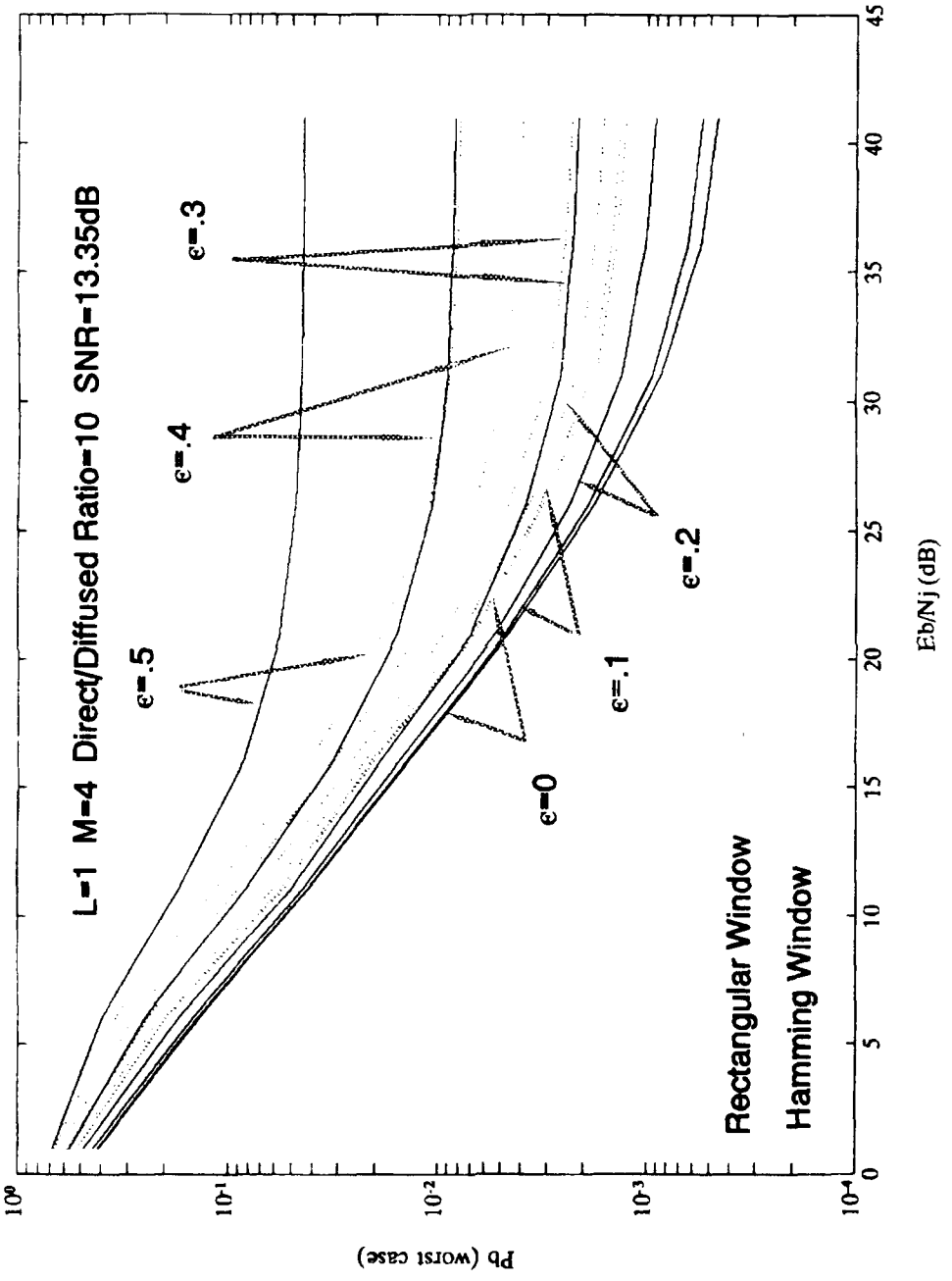

Figure 4.1: Worst case probability of bit error versus signal-to-jamming noise ratio for L=1, M=4, direct-to-diffuse ratio=10, and SNR=13.35 dB.

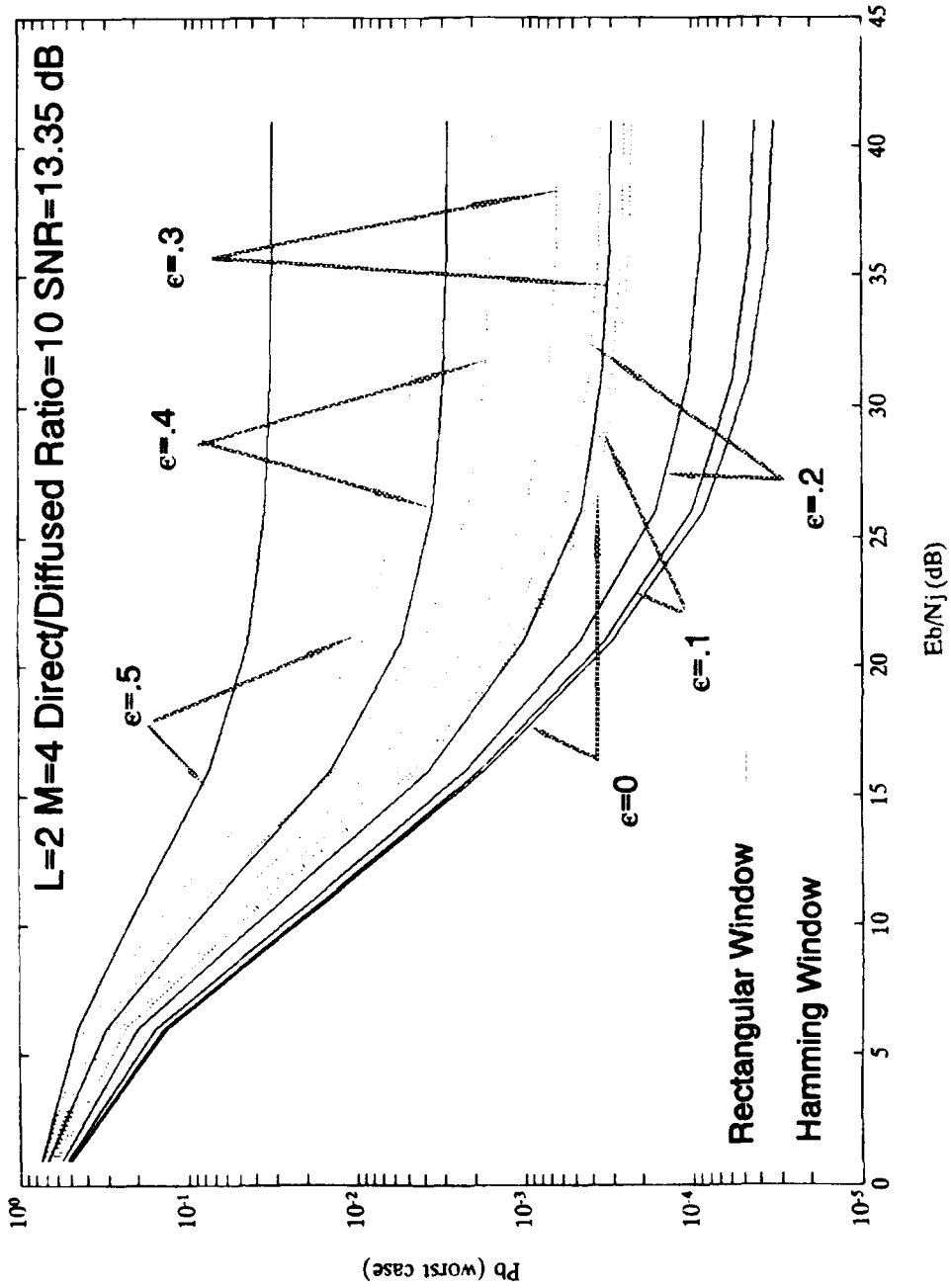

Figure 4.2: Worst case probability of bit error versus signal-to-jamming noise ratio for L=2, M=4, direct-to-diffuse ratio=10, and SNR=13.35 dB.

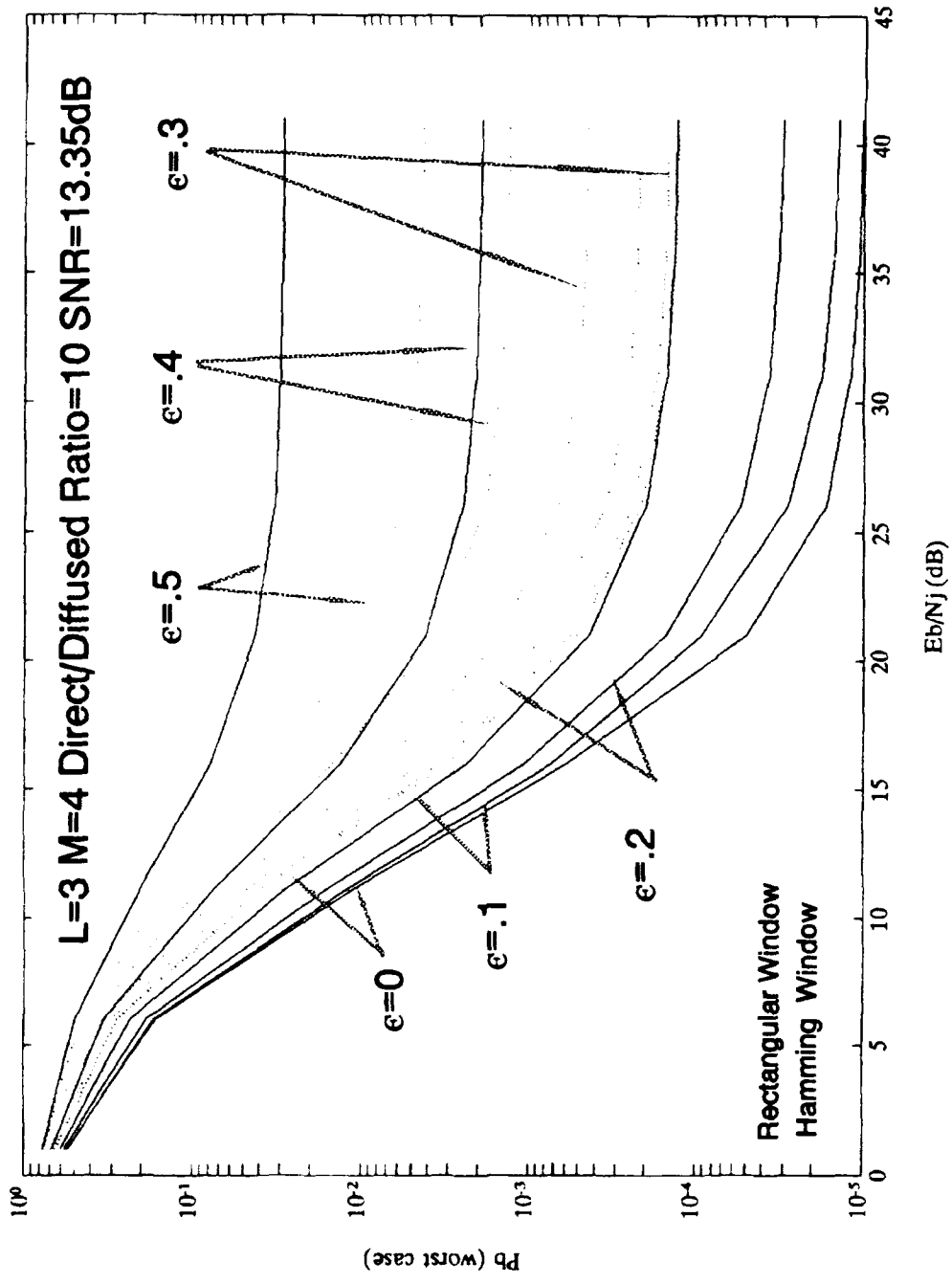

Figure 4.3: Worst case probability of bit error versus signal-to-jamming noise ratio for L=3, M=4, direct-to-diffuse ratio=10, and SNR=13.35 dB.

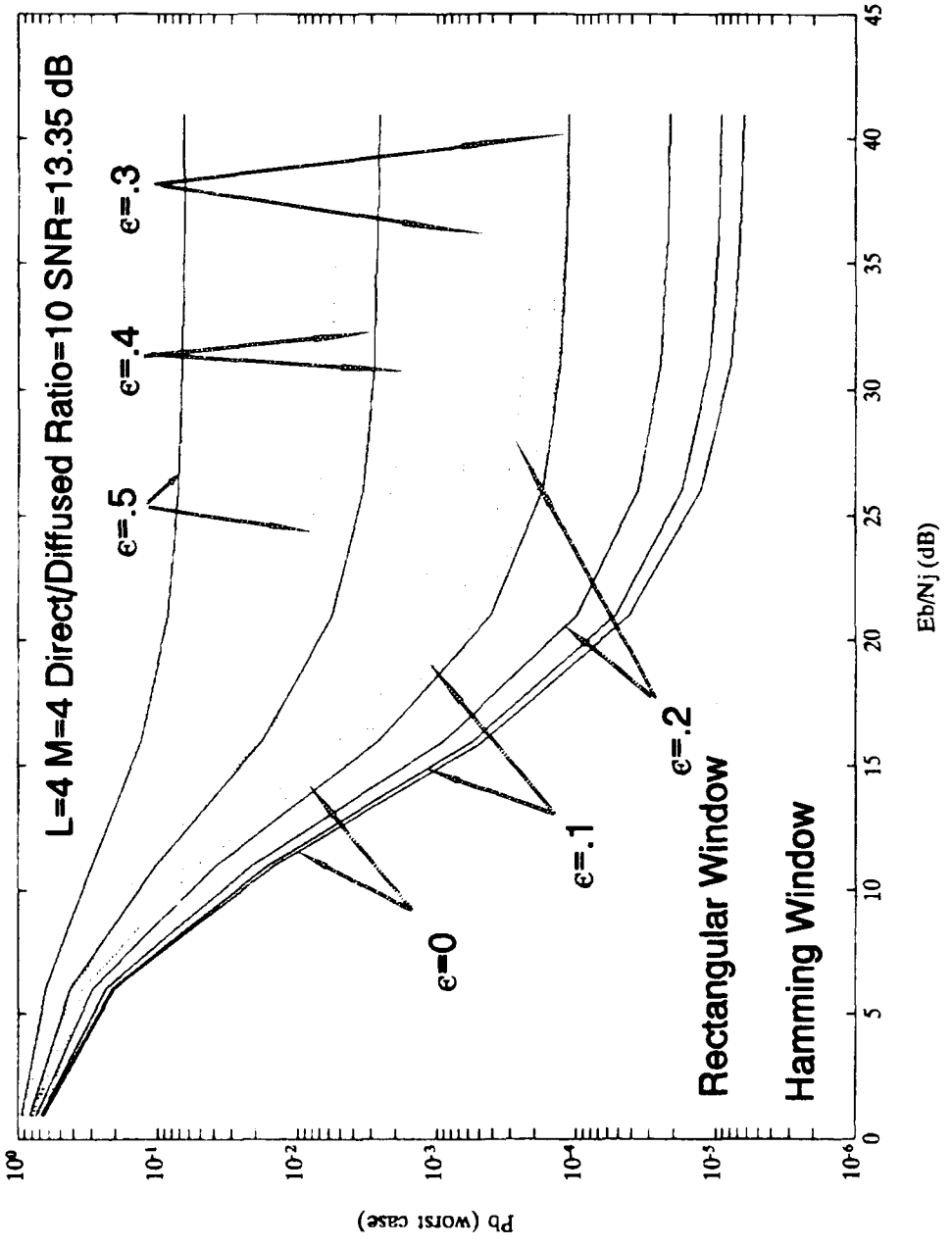

Figure 4.4: Worst case probability of bit error versus signal-to-jamming noise ratio for L=4, M=4, direct-to-diffuse ratio=10, and SNR=13.35 dB.

analyzes a conventional (non-DFT) noise-normalized MFSK receiver with quadratic detection. The results obtained here for the case of no Doppler shift (ε=0) and a rectangular window should be similar to those obtained in [4].

Differences in the results obtained in [4] and those obtained in this study are primarily due to the facts that the equivalent system bandwidths used in [4] and this thesis are different and the results in [4] are exact while the results in this study represent a union bound. The equivalent system bandwidth used in [4] is chosen to be minimal while the equivalent system bandwidth used in this work is chosen to enable increased frequency spacing between the DFT output bins as well as to allow comparisons to be made with the results in [1] and [2]. From this, it is expected that the data generated for this thesis will predict slightly worse performance than that predicted in [4]. This is observed in all cases.

Just as reported in [4], the performance of the DFT based communications system is enhanced as the number of frequency-hops per symbol is increased. This is especially true for the cases of little or no Doppler shift. For cases of large Doppler shift (i.e., ε=0.5), the performance of the receiver is slightly poorer as the hop rate is increased when non-uniform windowing is used. The error introduced by self-induced crosstalk overcomes the benefits usually associated with fast frequency-hopping. This is clearly seen in Fig. 4.1 and Fig. 4.4 for the case of a rectangular window and ε=0.5.

For E_b/N_j=41.0 dB, Pb=4.41x10^{-2} for a hop rate of one hop per symbol, and Pb=6.65x10^{-2} for a hop rate of four hops per symbol. The use of a Hamming window in this situation improves receiver performance as the number of hops per symbol increases, but the benefits are small compared to the complexities needed to implement a fast frequency-hopped receiver.

For the case of slow frequency-hopping, the results in Fig. 4.1 approach those reported in [2] as E_b/N_j becomes very large. This is expected because the decision statistic consists only of one component due to the fact that the carrier frequency is changed once per symbol. Furthermore, receiver performance degrades as either the jamming power or the Doppler shift increases. As reported in [1] and [2], the performance of the Hamming window is worse than that for a rectangular window for small Doppler shifts, but outperforms the rectangular window for large Doppler shifts. The value of ε at which the use of a Hamming window gives better performance than the use of a rectangular window (the crossover fractional frequency offset) is a function of the amount of jamming power at the receiver. At E_b/N_j=1.0 dB, for example, with a rectangular window, Pb=0.413 with ε=0 and Pb=0.687 with ε=0.5; while, with a Hamming window, Pb=0.524 with ε=0 and Pb=0.668 with ε=0.5. However, at E_b/N_j=41.0 dB, with a rectangular window, Pb=4.59x10^{-4} with ε=0 and Pb=4.41x10^{-2} with ε=0.5; while, with a Hamming window,

Pb=1.26x10^{-3} with ε=0 and Pb=7.87x10^{-3} with ε=0.5. For large Doppler shifts, the use of a Hamming window clearly improves receiver performance over a broad range of E_b/N_j.

This same phenomena exists for the cases of two, three, and four hops per symbol. In these cases, however, the larger hop rates have little effect on the value of the crossover fractional frequency offset. This is illustrated in Figs. 4.5 through 4.8 which plot the worst case probability of bit error as a function of the fractional frequency offset for E_b/N_j=16.0 dB and L=1,2,3 and 4. These results are summarized in Fig. 4.9, which plots the crossover fractional frequency offset as a function of the hop rate for various values of E_b/N_j. As can be seen, the values of the crossover fractional frequency offset remain in a small band for each value of E_b/N_j, and increase as the amount of jamming power at the receiver increases.

From Fig. 4.9, it can be seen that the crossover fractional frequency offset does not follow a smooth curve as the hop rate is varied. In viewing these curves, it must be remembered that the results in Figs. 4.1 through 4.4 represent the worst case performances of union bound solutions. These worst case results are obtained by varying the value of the fraction of spectrum jammed (γ) and retaining only the worst case performance. The value of γ giving worst case performance at one hop rate is not generally the same value at a different hop rate. The fact that only a representative number of

discrete values of γ are used to approximate the continuous range of possible γ's contributes to this situation.

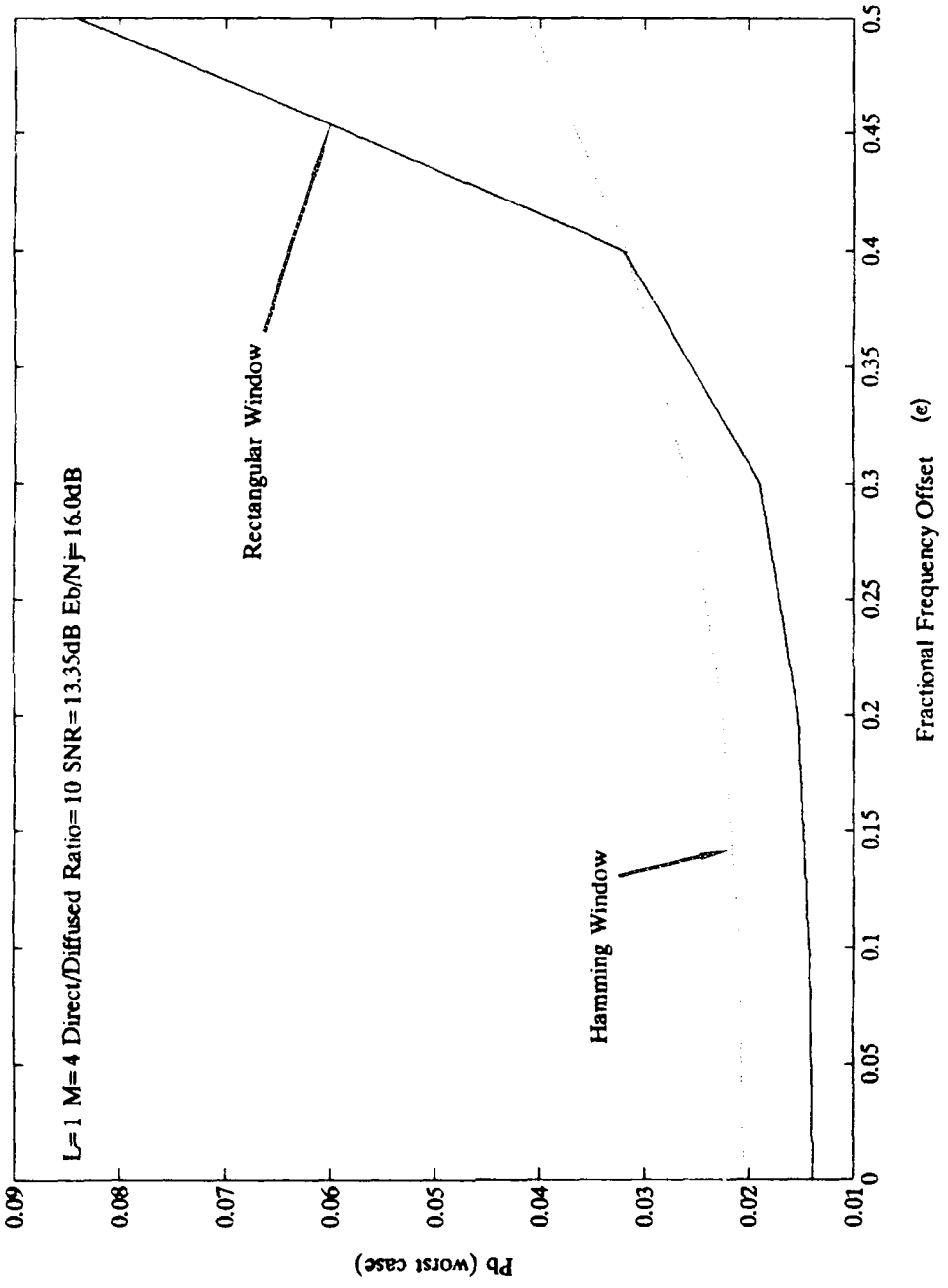

Figure 4.5: Worst case probability of bit error versus fractional frequency offset for the case of L=1, M=4, SNR=13.35 dB, and E_b/N_j=16.0 dB.

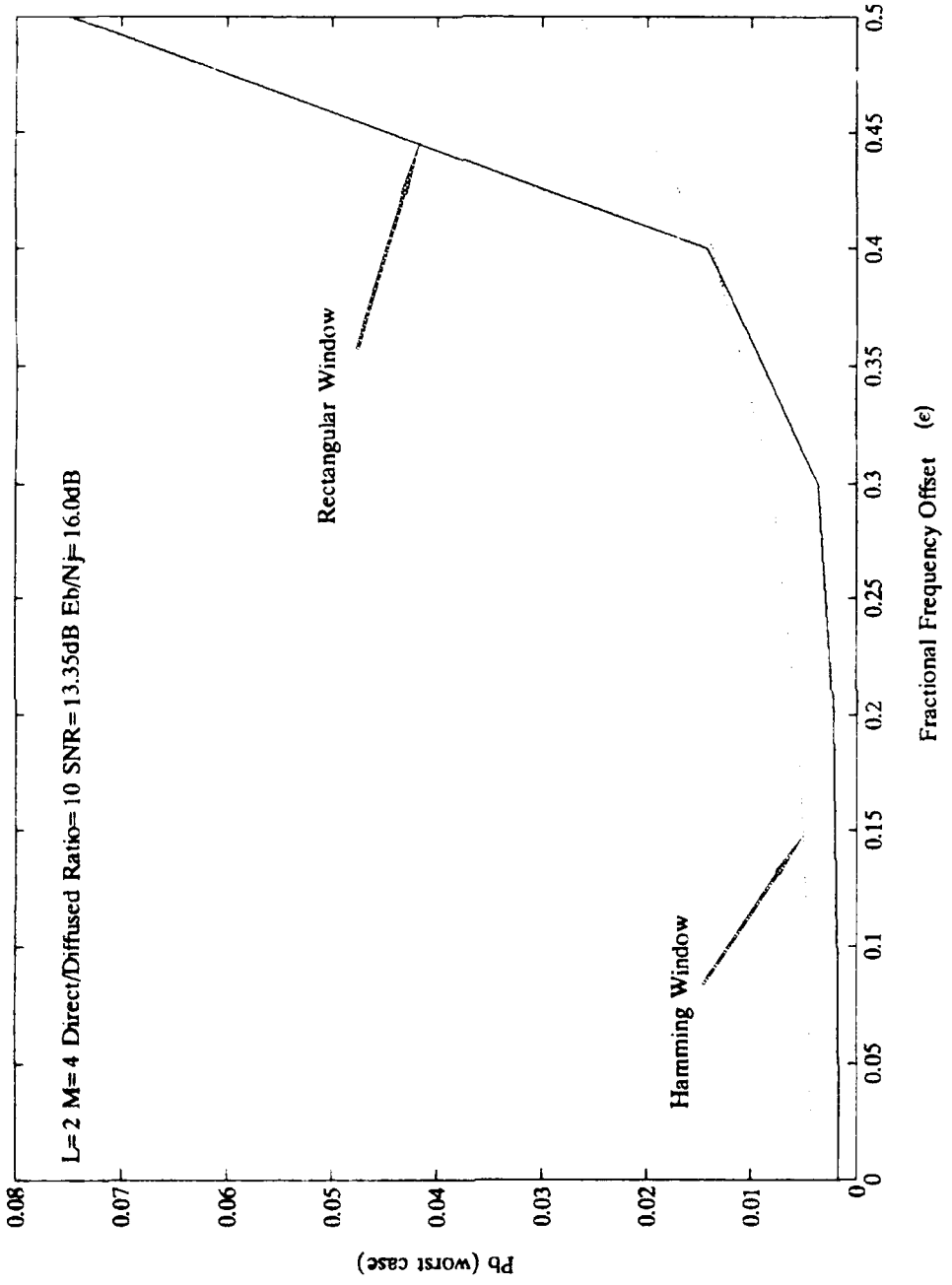

Figure 4.6: Worst case probability of bit error versus fractional frequency offset for the case of L=2, M=4, SNR=13.35 dB, and E_b/N_j=16.0 dB.

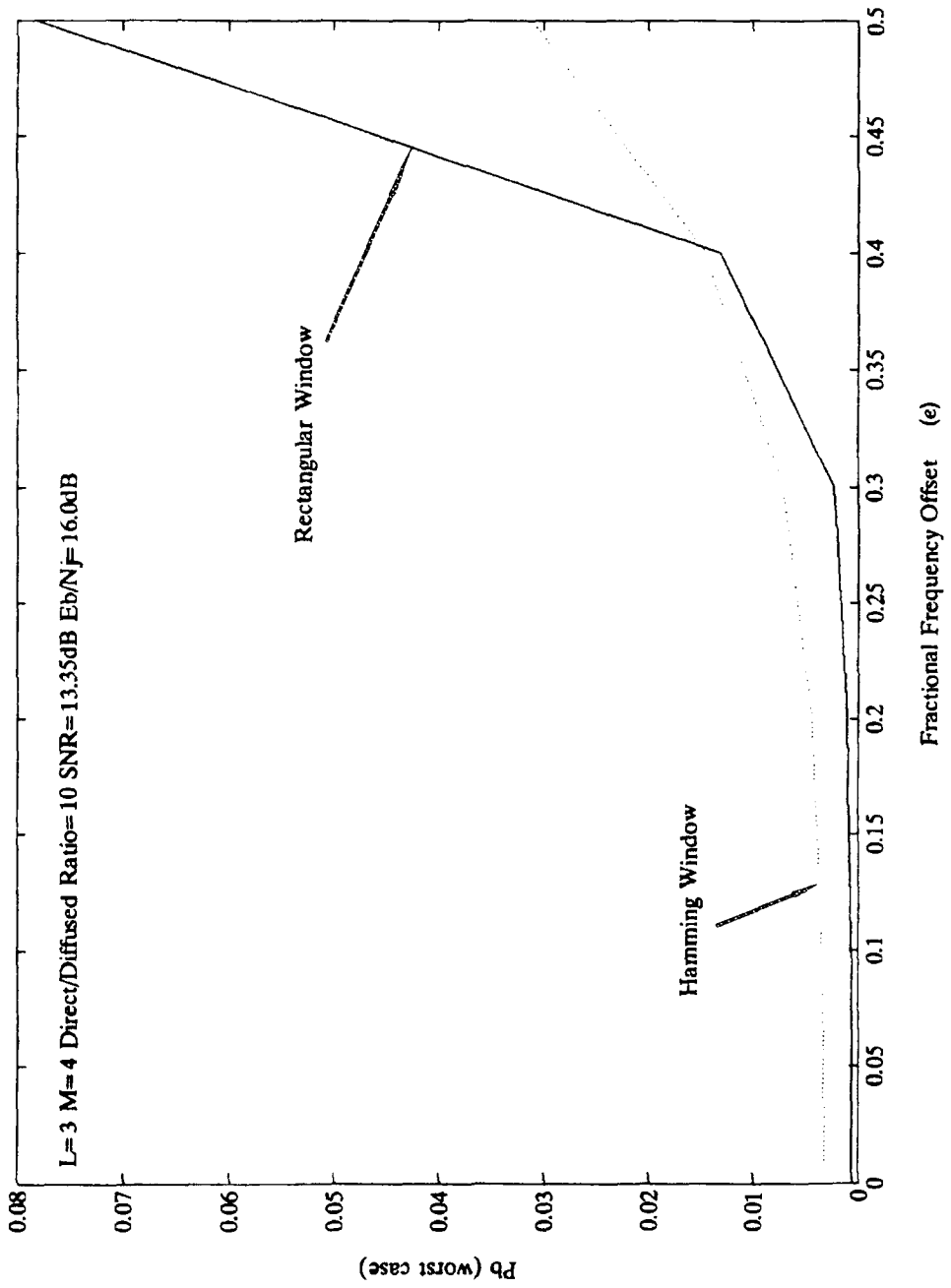

Figure 4.7: Worst case probability of bit error versus fractional frequency offset for the case of L=3, M=4, SNR=13.35 dB, and E_b/N_j=16.0 dB.

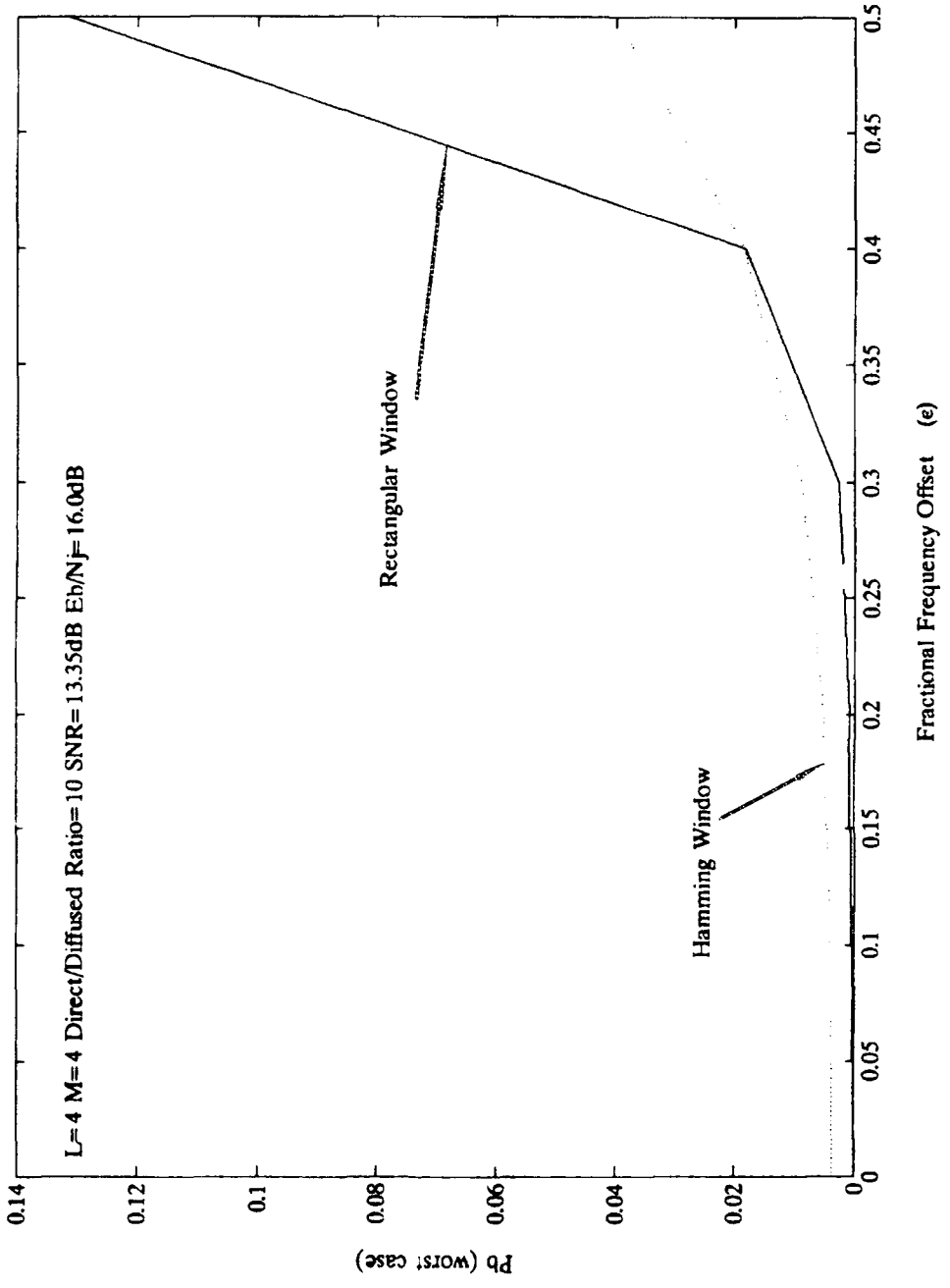

Figure 4.8: Worst case probability of bit error versus fractional frequency offset for the case of L=4, M=4, SNR=13.35 dB, and E_b/N_j=16.0 dB.

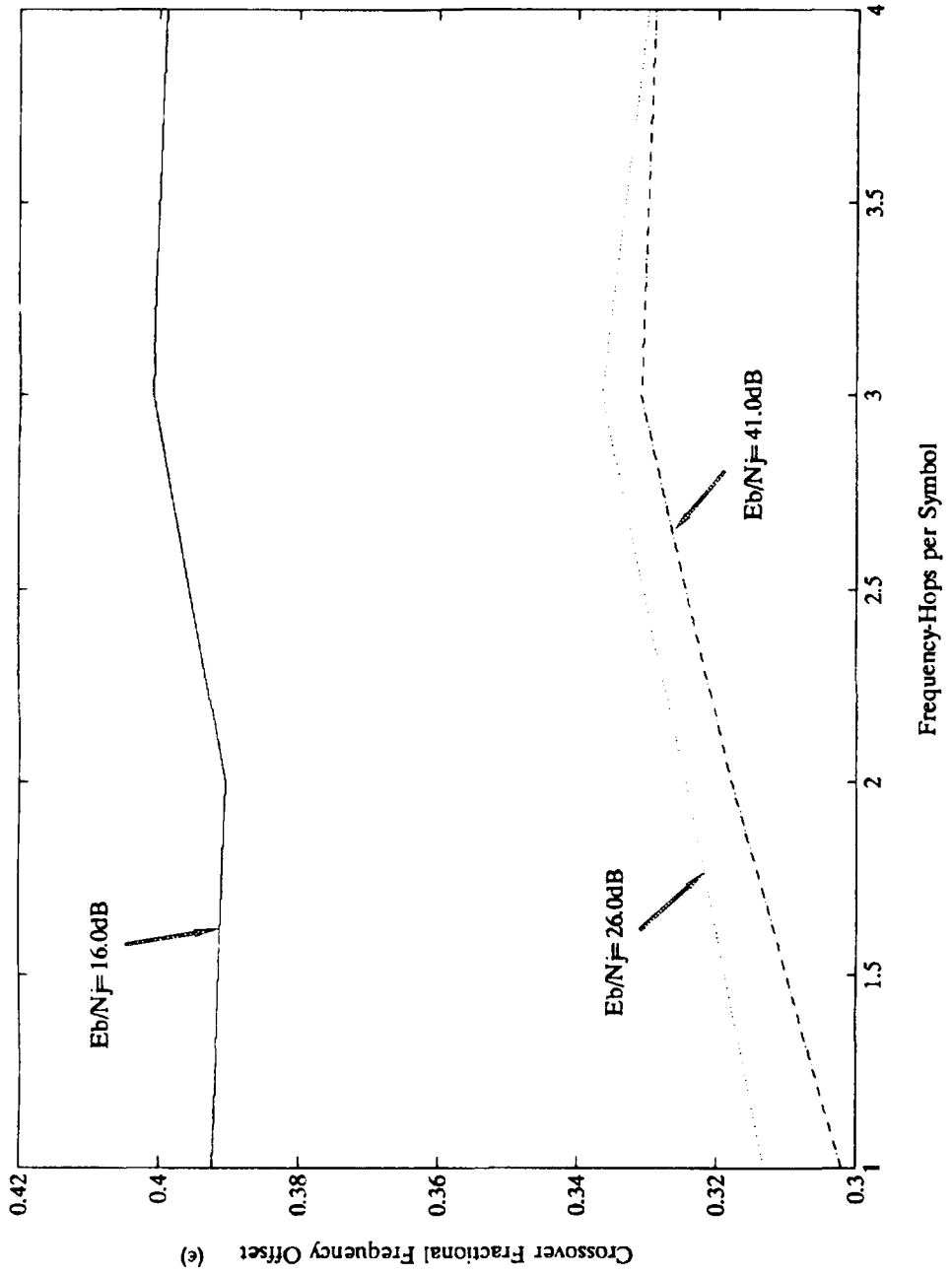

Figure 4.9: Crossover fractional frequency offset versus frequency-hops per symbol for the case of M=4, and SNR=13.35 dB.

V. CONCLUSIONS AND RECOMMENDATIONS

As the frequency-hop rate of the DFT based communications system with noise-normalization increases, receiver performance improves in the absence of large Doppler shifts. However, when large Doppler shifts exist, the errors introduced as a result of self-induced crosstalk counteract any benefits gained from the use of fast frequency-hopping. The advantages gained by using a non-uniform window in the presence of large Doppler shifts improve the situation, but not enough to warrant the added hardware complexities inherent to the application of fast frequency-hopped spread spectrum.

The amount of Doppler shift necessary to warrant the use of a non-uniform window is primarily a function of the jamming noise power spectral density. Holding all else constant, as N_j increases, the amount of Doppler shift necessary to justify the use of a non-uniform window increases. At very small values of E_b/N_j the use of a non-uniform window results in degraded performance for all but the most extreme Doppler shifts. The performance degradation resulting from using a non-uniform window in a situation with little Doppler shift, however, is small compared to the performance enhancement gained by using a non-uniform window when large Doppler shifts exist. In general, in the absence of all information regarding

the nature of the received signal, the use of a non-uniform window is preferred in all situations.

For all but the most severe conditions of Doppler shift and jamming power, the receiver studied in this thesis provides reliable communications through the use of fast frequency-hopped spread spectrum. Communications reliability does not come without a price. The complexities involved in implementing a fast frequency-hopped spread spectrum system are enormous and are not worth the benefits in all situations. As an example, in order to keep the same number of samples per frequency-hop for the DFT, the total symbol duration time becomes a linear function of the hop rate. In this thesis the hop time is determined to be equal to one second. For the case of one frequency-hop per symbol, this translates to a symbol duration time of one second, but for the case of L frequency hops per symbol, this translates to a symbol duration time of L seconds. Thus, a faster frequency-hop rate translates to slower, but in many situations, more reliable communications.

Despite its drawbacks, the use of the DFT based receiver may be superior in situations where the content of the message is more valuable than the speed of delivery. By employing the DFT based receiver with fast-frequency hopping, a system can be developed which has the potential to deliver reliable communications with considerable anti-jam protection. Situations relying on this type of communications protection are common in the military environment.

In order to gain deeper insight into the relationships between the fractional frequency offset, the modulation order, the hop rate, and the signal energy-to-jamming noise power spectral density ratio, further study should be conducted. This study should emphasize the changes in the crossover fractional frequency offset observed while varying the key parameters listed above. Also, the calculation of the exact solution is possible, and should be utilized in any further study. Due to limited computational resources, this was not possible in this thesis.

Finally, the work presented here is theoretical in nature and should be tested with actual hardware. The assumptions made in this analysis were selected to ease the burden of computational effort needed to solve the problem. They may not correspond to actual conditions needed for optimal communications in a real world system. Only building this receiver and testing it under realistic conditions will prove or disprove the usefulness of the DFT based, noise-normalized receiver.

LIST OF REFERENCES

1. Richard A. Yost, "On Nonuniform Windowing M-ary FSK Data in a DFT Based Detector," *IEEE Trans. on Communications*, Vol. COM-28, No. 12, pp. 2014-2019, December 1980.

2. Chris G. Kmiecik, *Effects of Non-Uniform Windowing in a Rician-Fading Channel and Simulation of Adaptive Automatic Repeat Request Protocols*, Master's Thesis, Naval Postgraduate School, Monterey, California, June 1990.

3. Charles E. Cook and Howard S. Marsh, "An Introduction to Spread Spectrum," *IEEE Communications Magazine*, Vol. 21, No. 2, March 1983.

4. Thomas M. Clemons III, R. Clark Robertson, and Tri T. Ha, "Error Probabilities of Frequency-Hop MFSK with Noise-Normalization Combining in a Fading Channel with Partial-Band Interference", paper presented at the IEEE Global Telecom Conference and Exhibition, San Diego, California, 3 December 1990.

5. Anthony D. Whalen, *Detection of Signals in Noise*, pp. 104-105, Academic Press, 1971.

6. Alberto Leon-Garcia, *Probability and Random Processes for Electrical Engineering*, pp. 386-387, Addison-Wesley Publishing Company, 1989.

7. I.S. Gradshteyn and I.M. Ryzhik, *Table of Integrals, Series and Products*, pp. 718 and 961, Academic Press, 1980.

8. Athanasios Papoulis, *Probability, Random Variables, and Stochastic Processes*, p. 95, McGraw-Hill Book Company, 1984.

9. Robert D. Strum and Donald E. Kirk, *First Principles of Discrete Systems and Digital Signal Processing*, pp. 389-392, Addison-Wesley Publishing Company, 1989.

10. M. Abramowitz and I. A. Stugun, *Handbook of Mathematical Functions*, p. 486, Dover Publications, 1972.

11. *Tables of Integral Transforms*, vol. 1, p. 245, McGraw-Hill Book Company, 1954.

12. Jon Mathews and R.L. Walker, *Mathematical Methods of Physics*, The Benjamin/Cummings Publishing Company, 1970.

INITIAL DISTRIBUTION LIST

1. Defense Technical Information Center — 2
   Cameron Station
   Alexandria, Virginia 22304-6145

2. Library, Code 52 — 2
   Naval Postgraduate School
   Monterey, California 93943-5002

3. Chairman Code EC — 1
   Department of Electrical and
   Computer Engineering
   Monterey, California 93943-5000

4. Prof. R. C. Robertson, Code EC/Rc — 5
   Department of Electrical and
   Computer Engineering
   Monterey, California 93943-5000

5. Prof. T. T. Ha, Code EC/Ha — 1
   Department of Electrical and
   Computer Engineering
   Monterey, California 93943-5000

6. LT Thomas W. Vece — 2
   Naval Submarine School
   Box 700
   Groton, Connecticut 06349-5700